Modeling and Electronic Characterizations of Carbon Nanotube Field Effect Transistors

Maryam Etezadbrojerdi

A Thesis
in
The Department
of
Electrical Engineering

Presented in Partial Fulfillment of the Requirements
for the Degree of Master of Applied Science (Electrical Engineering) at
Concordia University
Montreal, Quebec, Canada

March 2006

© Maryam Etezadbrojerdi, 2006

Library and Archives Canada

Published Heritage Branch

395 Wellington Street
Ottawa ON K1A 0N4
Canada

Bibliothèque et Archives Canada

Direction du Patrimoine de l'édition

395, rue Wellington
Ottawa ON K1A 0N4
Canada

Your file Votre référence
ISBN: 0-494-14256-1
Our file Notre référence
ISBN: 0-494-14256-1

NOTICE:
The author has granted a non-exclusive license allowing Library and Archives Canada to reproduce, publish, archive, preserve, conserve, communicate to the public by telecommunication or on the Internet, loan, distribute and sell theses worldwide, for commercial or non-commercial purposes, in microform, paper, electronic and/or any other formats.

The author retains copyright ownership and moral rights in this thesis. Neither the thesis nor substantial extracts from it may be printed or otherwise reproduced without the author's permission.

AVIS:
L'auteur a accordé une licence non exclusive permettant à la Bibliothèque et Archives Canada de reproduire, publier, archiver, sauvegarder, conserver, transmettre au public par télécommunication ou par l'Internet, prêter, distribuer et vendre des thèses partout dans le monde, à des fins commerciales ou autres, sur support microforme, papier, électronique et/ou autres formats.

L'auteur conserve la propriété du droit d'auteur et des droits moraux qui protège cette thèse. Ni la thèse ni des extraits substantiels de celle-ci ne doivent être imprimés ou autrement reproduits sans son autorisation.

In compliance with the Canadian Privacy Act some supporting forms may have been removed from this thesis.

While these forms may be included in the document page count, their removal does not represent any loss of content from the thesis.

Conformément à la loi canadienne sur la protection de la vie privée, quelques formulaires secondaires ont été enlevés de cette thèse.

Bien que ces formulaires aient inclus dans la pagination, il n'y aura aucun contenu manquant.

Abstract

Modeling and Electronic Characterizations of Carbon Nanotube Field Effect Transistors

Maryam Etezadbrojerdi

Nanodevices -due to their nanoscale size- exhibit novel physical, chemical or biological properties. Transistors are being scaled to a regime, in which quantum mechanical phenomena are beginning to affect their performances. Since Field Effect Transistors performance eventually will be degraded by quantum effect, it is important to explore alternative devices which operate based on quantum effect. A whole range of possible device concepts have been proposed by scientists. Carbon nanotubes (CNTs) offer a technology with an exciting solution to the scaling issues of transistors and interconnects. The goal of the present work is to explore the concept of nanotechnology, carbon nanotubes and its function in Carbon Nanotube Field Effect Transistor (CNFET) and develop an analytical theory for nanometer-size field-effect transistor. This thesis research models and characterizes the future opportunities of CNFETs within digital designs.

The energy band of CNFETs has been modeled at equilibrium. For equilibrium condition, the carrier concentration is found by allowing the local electrostatic potential to rigidly shift the carbon nanotube density of states. The effect of contacts characteristics leading to the potential spikes in the tube at the source and drain of height determined by both work functions of source and drain and V_{gs} have been explored.

By approximating the potential barrier shape and using Landauer-Büttiker expression it can be seen that CNFET have noteworthy IV characteristics. The current characteristics are similar to MOSFETs, having the operation being controlled by the electric field from the gate and source/ drain voltage which can lead to strong band bending allowing carriers to tunnel through the interface barrier. This can show that CNFETs have prominent potential to replace the current Field effect transistors

Acknowledgment:

I would like to thank Dr.Kahrizi for giving me the opportunity to work on this project and in his group; his advice, comments, support, and contacts have been invaluable. I have learned an enormous amount in the last two and a half years. Dr.Kahrizi's discussions and advice on the topic were very helpful and his comments on my thesis were especially enlightening.

I would also want to thank Dr.Rossokhaty. Getting to know him and learn from him was one of the highlights of my studies at Concordia University. His thoughts and memories will always be in my heart. I guess this is the reason that I have not still grasped the fact that he is not among us anymore. I am and always will be honored that I was one of his students.

I would like to thank David L. John from University of British Columbia and Dr. Supriyo Datta from Purdue University. Their emails and comments on the subject were incredibly helpful. It was wonderful to have the perspective and knowledge of people working first hand within the nanotube field. I would also like to thank Dr.Kahrizi's research group past and present. They gave me help, comments and friendships. It was a pleasure working in the same lab with them.

And last but not least, I would like to thank my family. My dad and mom have gotten me through everything, good and bad. I do not know how to thank them enough. It seems the more I grow up, the more help and advice I ask for. No distance will ever be great enough to keep me from calling home everyday and sometimes even a few times a day.

Thank you also to my brother Mohammad, my best friend who has shown me how to follow my dreams and kept me calm through everything.

Contents

1 Introduction

1.1 Background of Nanotechnology and Nanoelectronics 1

1.2 Nanotechnology and nanoelectronics..3

1.3 Strategies to make smaller devices...4

1.4 Technology scaling...8

1.4.1 Technology scaling challenges..9

2 Carbon based material and nanotubes..15

2.1 Carbon atoms...15

2.1.1Hybridization in Carbon Atoms 15

2.2 Carbon materials..16

2.2.1 Graphite..17

2.2.2 Buckyballs...18

2.2.3 Carbon nanotubes..19

2.3 Structure of Single-Wall Carbon Nanotubes 20

2.3.1 Classification of carbon notubes..22

2.3.2 Synthesis of carbon nanotubes...26

3 Carbon Nanotubes Applications..30

3.1 Mechanical Application...30

3.2 Electronics Application...31

3.3 Advantages of Using Carbon Nanotubes over Silicon Wires.................................32

3.3.1 Selecting Semiconducting notubes....33

4 Carbon Nanotube Field Effect Transistors (CNFET)....35

Transistor Based on a Single Carbon Nanotube....35
Schottky Barrier Field Effect Transistors....36
4.2.1 Fabrication....36
4.2.2 Operation....40
The impact of the channel thickness on CNFET characteristics....43

5 CNFET under equilibrium Condition....47

5.1 Carbon Nanotube Electrostatics....48
5.2 Concentration of Electrons....50
5.3 Concentration of holes....56
5.4 The energy diagram of the conduction band without using the Maxwell-Boltzmann approximation....63
5.5 Energy band diagram using Maxwell-Boltzmann approximation....67

6 CNFET under non-equilibrium condition....69

6.1 Transmission coefficient at source/drain of a CNFET....71
6.1.1 Transmission Coefficient at Source/-carbon nanotube junction of a CNFET..73
6.1.2 Transmission coefficient at drain-carbon nanotube junction of a CNFET......75
6.2 I-V Characteristics of CNFET....79

7 Conclusions, contributions....84

List of Figures:

1-1 Number of transistors per processor as a function of time.

1-2 The year of introduction of microprocessors versus MIPS.

1-3 Principle of contact printing.

1-4 Dip pen nanolithography.

1-5 Scanning Tunneling Microscope.

1-6 Sub-threshold leakage versus temperature.

1-7 A 90 nm MOS transistor with the 50 nm channel with the 1.2 nm gate dielectric.

1-8 Energy to do the logic operation vs. different technology generation.

1-9 Sub-Wavelength Lithography.

1-10 Heat Flux and Temperature Variation on the chip.

2-1 Layers of Graphite Shits.

2-2 The unrolled honeycomb lattice of the nanotube.

2-3 Band structure of graphene.

2-4 Carbon nanotube cylinders with varying chiralities.

2-5 The schematic diagram for the arc-electric discharge method as developed by Saito in 1995.

3-1 Multi walled carbon nanotubes and single walled carbon nanotubes.

4-1 Carbon nanotube transistor on Sio2 substrate using gold as source and drain.

4-2 Top view of the CNFET with Sio2 substrate and gold source and drain.

4-3 Electrodes patterned on top of the CNT.

4-4 Top gated CNFET.

4-5 Au-contacted p-FET converted to n-FET by annealing.

4-6 Hole current dominates in the system for high negative voltage.

4-7 The energy diagram of the CNFET.
4-8 Energy band bending of a CNFET with different gate oxides.
4-9 Drain current versus gate voltage for two different diameters of nanotubes.
5-1 Two types of nanotube /metal contacts: (a) nanotube side contacted by the metal by Van der Waals adhesion; (b) nanotube end bonded to the metal (covalent/metallic bonding).
5-2 CNFET Structure.
5-3 A one dimensional array of allowed quantum states in k space.
5-4 Electron density at the mid band of the carbon nanotube versus gate voltage where Maxwell-Boltzmann approximation is applicable.
5-5 Hole density at the mid band of the carbon nanotube versus Gate voltage where Maxwell-Boltzmann approximation is applicable.
5-6 Energy band diagram versus charge density of a metal-carbon nanotube junction.
5-7 Electron density at the mid band of the carbon nanotube versus gate voltage where Maxwell-Boltzmann approximation is not applicable.
5-8 Energy band diagram near the source end without using the Maxwell-Boltzmann approximation.
5-9 Energy band diagram near the source end without using the Maxwell-Boltzmann approximation considering the work function of carbon nanotube being equal to 4.2 eV, V_{gs}=0.3 and $\Phi_S=\Phi_D$ set to 4.5 eV and 4.33 eV.
5-10 Energy band diagram near the source end using the Maxwell-Boltzmann approximation
considering the work function of carbon nanotube being equal to 4.2 eV, V_{gs}=0.3 and $\Phi_S=\Phi_D$ set to 4.5 eV and 4.63 eV.
6-1 Band diagrams along the nanowire channel from source to drain for positive gate bias and positive drain bias VD>0.

6-2 Conduction energy band diagram for various bias conditions.

6-3 Schottky barrier at the source end of the CNFET.

6-4 The energy diagram of the CNFET at non-equilibrium condition.

6-5 The computed I_d vs. V_{ds} characteristic with gate biases Vgs=0.32-0.37 V, 0.4 V for CNFET.

6-6 Current Characteristic of carbon nanotube for CNFETS at non-equilibrium when V_{ds}=0.2 v and V_{gs} changes from 0.32 to 0.39 volts.

6-7 Switching in carbon nanotubes in CNFETS, linear region for small V_{ds} in the output characteristics and saturation for large enough V_{ds}. (experimental results).

Chapter 1
Introduction

1.1 Background of Nanotechnology and Nanoelectronics:

The semiconductor Industry Association (SIA) has been publishing roadmaps for semiconductor technology since 1992.These roadmaps, taking history as a guide; represent a consensus outlook of industry trends. The recent roadmaps incorporate participation from the global semiconductor industry; including the United States, Europe, Japan, Korea, and Taiwan. They basically affirm the desire of the industry to continue with Moore's law, which is often stated as doubling of transistor performance and quadrupling of the number of devices on a chip every two or three years.

Microelectronics has been around since early 1960. Although in 1961 there were only a handful number of transistors on each chip, in 1965 Gordon Moore- the cofounder of the Intel Corporation-predicted in a bold statement that the number of transistors in the integrated circuits as a function of time would increase exponentially for the foreseeable future and he added that although no exponential is forever but we can delay 'forever', see Fig.1-1.

The phenomenal progress signified by Moore's law has been achieved through scaling of the metal-oxide-semiconductor field effect transistor (MOSFET) from larger physical dimensions to smaller physical dimensions, thereby gaining more speed and density. In the past 40 years, MOSFET has become the basic building block for almost all computing devices. The steady growth of their popularity is due to the steady shrinking of the feature size which at the present has reached 55 nm.

Silicon wafers are divided into chips which consist of many electronics devices. The basic block for an electronic device is a transistor which is about a billion on each chip.

The smallest feature in a transistor is called channel; therefore, by making the channel smaller the whole transistor becomes smaller.

By each technology generation, which is 18 months to 2 years, this dimension shrinks by a factor of $\frac{L}{\sqrt{2}}$ and consequently the area drops by the factor of 2 .This means that twice as many device fits on the each chip and makes it twice powerful. The goal and challenge in terms of MIPS (millions of structure delivered per second) is now to have one TIPS (tera instructions per second) by the end of the decade, see Figure 1-2.

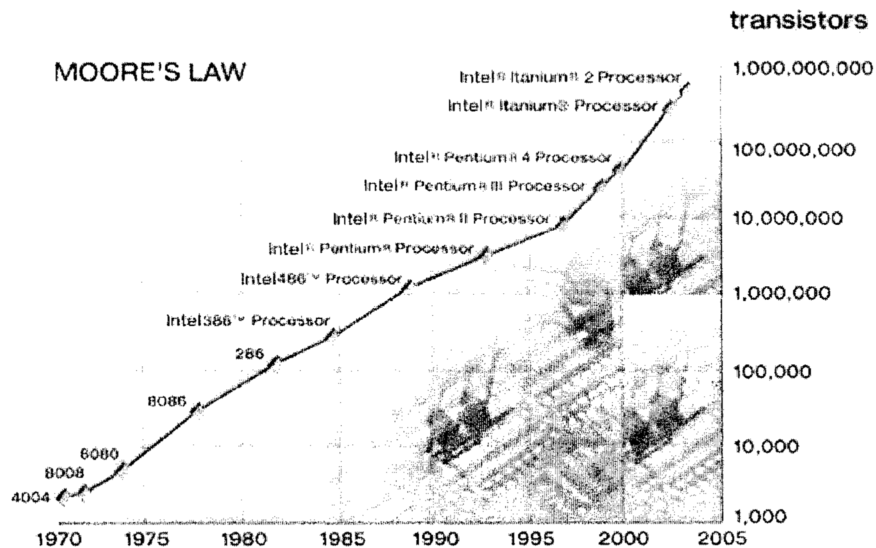

Figure 1-1: The plot shows the number of transistors per processor as a function of time [1].

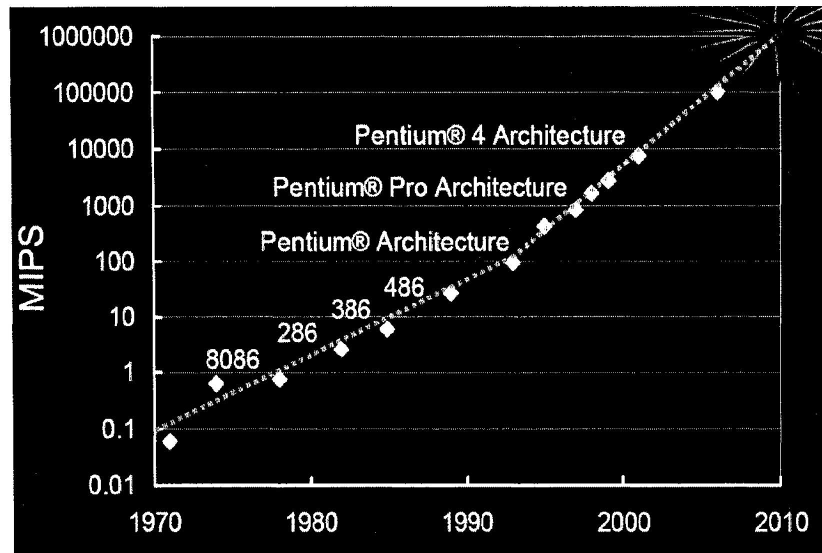

Figure 1-2: The x access shows the year of introduction of microprocessors and the y axis shows MIPS (millions of structure delivered per second) up to Pentium 4 [2].

1.2. Nanotechnology and Nanoelectronics

Nanotechnology relates to the creation of devices, structures and systems whose size range from 1 to 100 nanometer (nm). Nano comes from the Greek work nanos which means dwarf. For comparison, 10 nanometer is 1000 times smaller than the diameter of human hair, a DNA is about 2nm and atoms are less than a nanometer in diameter. Nanometer devices, due to their nano scale size, exhibit novel physical, chemical or biological properties.

A famous lecture in 1959 by Nobel Prize winning physicists Richard Feynman was titled," There is plenty of room at the bottom" was given to stimulate new discoveries and capabilities at the atomic and molecular scale; however, not much happened until the 1980s when the scanning tunneling microscope and other sophisticated instruments emerged. Nanotechnology is nowadays a hot topic and suitable to be thought in various educational level.

One of the obvious places where miniaturization has had a dramatic impact is, fabricating smaller electronic devices which have led to the dramatic improvement in computers performances as a function of time .Today, the question that often is asked is that: aren't computers small enough today. Bill gates in 1981 said:"640K ought to be enough for anybody", he referred to the memory of the computers at that time. Even Bill Gates who was the visionary for computers thought in 1981 that maybe we have enough memory for our computers. Now in 2005 with 640 K we can find calculators or wrist watches. So we can say that one of the motivations to make things smaller is that the definition of small has been changing in the last couple of decades.

In the last decade, we have seen the significant progress in every aspect of nanotechnology: nano particles and powders, electrical, optical, mechanical nano devices and nanostructure biological materials. A scientific and technical revolution has just begun based upon the ability to systematically organize and manipulate structures at nanoscale. Payoff is anticipated within the next 10-15 years.

1.3. Strategies to make smaller structures:

There are two general strategies to make smaller structures:

1) Top down approach

2) Bottom-Up approach

1) Top-Down approach:

In this approach we start with a bigger structure and chisel away the material to make nanoscale objects.

Examples:

1) Photolithography

Photolithography is limited to the wavelength of light. Nowadays with the best optical instruments, we can only pattern down to 100nm using this approach. Other energy sources besides light are used today to make smaller pattern, for example sources like electron beam which can make 10 nm or sub 10nm length scale.

2) Nanoimprint Lithography (NIL):

The advantage of this lithographic technique is the ability to pattern sub-25 nm structures over a large area with a high-throughput and low-cost. Imprint lithography can be used for low-cost mass production of nanostructures.

For this technique, first a layer of resist like a polymer or plastic layer is put on the substrate. When heated up above the glass transition temperature of the polymer, the pattern of the mold is pressed into the melted polymer film. After being cooled down, the mold is separated from the sample and the pattern resist is left on the substrate. Typically, the intrusion of the mold is from 40 to 200 nm and the thickness of the resist is from 50 to 250 nm. The resist should be kept thicker than the mold intrusion to prevent the mold from contacting the substrate.

3) Microcontact Printing:

A very common strategy which puts together the two methods of top down and bottom up is microcontact printing .This method only delivers the molecules at particular locations.

The idea is similar to ink stamping. We take the stamp which is patterned and coat it with an ink which - just like the ink on the surface- can roll the molecules on the surface. Molecules will form these well defined aggregates at the points where are in contact with the surface in micron or submicron length scales, see Figure 1-3.

Microcontact printing is a very powerful method for surface structuring. Patterns can be made on many different materials and on flat or curved surfaces. Repeated printing, using different stamps, can be used to make complex surface patterns of more than one kind of molecule.

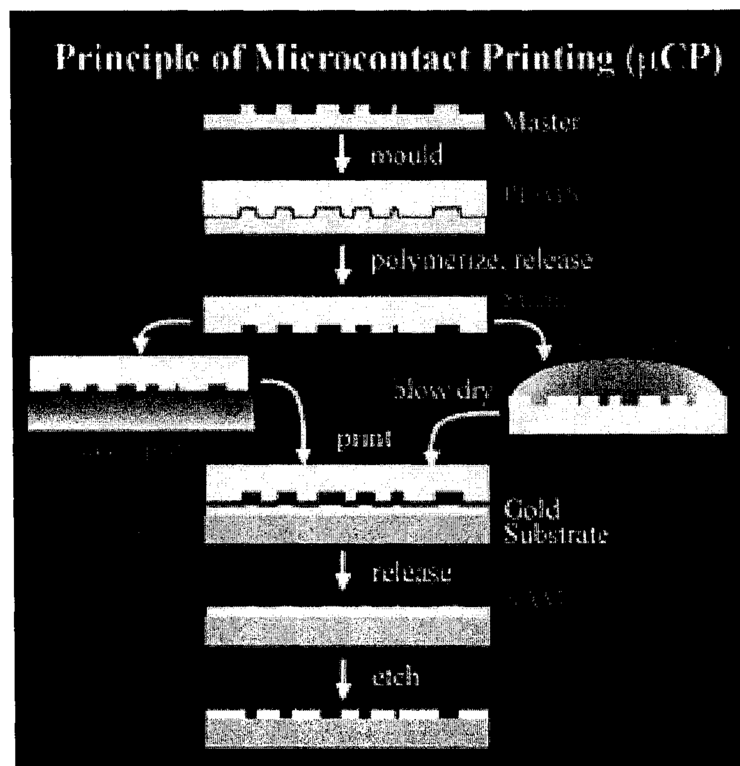

Figure 1-3: Principle of contact printing. [3]

4) Nanosphere Lithography:

For this method we should start with a clean substrate and then coat it with a solution which contains small spheres in the scale of microns or hundred nanometers. These spheres will assemble in to a tight pattern similar like racking balls in billiard. There are arrays of small triangles in the length scale of 100 nm or less among the spheres in the solution which can be filled by a desirable solution and then by lifting off the spheres the nanometer size pattern can be achieved.

2) Bottom-Up approach:

In this approach the small entities get assembled to larger objects in nanometer scale.

Examples:

1) Carbon nanotube synthesis:

One way to make nanotubes is to flow carbon molecules in to a furnace under the appropriate condition, so spontaneously bottom up approach takes place.

2) Molecular Self-Assembly:

In biology, at molecular length scale, self-assembly is very common .For example protein can be spontaneously folded in to complicated structures. The fundamental laws of nature (for example thermodynamics) are driving this process. The problem with this method is that it is relied on self assembly and this assembly has to get directed.

3) Dip Pen Nanolithography:

In Dip Pen Lithography the molecules are left behind when the tip slides on top of the surface just like when pen leaves behind the ink on the surface, see Figure 1-4. The only challenge here is to make the tip as sharp as possible.

These tips nowadays are made with radius of curvature of about 10 nanometers.

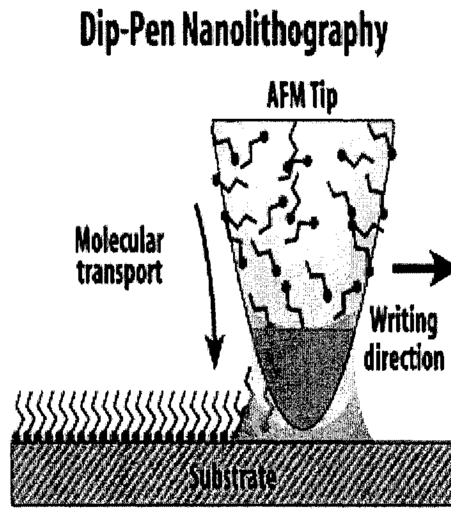

Figure 1-4: Dip pen nanolithography. [4]

4) Nanolithography with ultra-high Vacuum Scanning Tunneling Microscopy:

Scanning Tunneling Microscope (STM) works by scanning the sharp tip over the surface of a sample. The tip should be close to the surface, but not yet touch it. By applying a voltage between the sample and tip, current will flow between the two. This current is known as the tunneling current and hence the device is called scanning tunneling microscope, see Figure 1-5. This current depends very sensitively on the distance between the tip and the surface. If the distance between the tip and the sample changes by the tenth of the nanometer, about the length scale of the individual of atom, the current will change by the factor of ten. By increasing the voltage between the tip and the sample we can increase the energy of incident electrons. About some energy (electrons' energy threshold), these electrons start to damage the surface and may break chemical bonds between the atoms.

So in order to prevent it, what has to be done was to coat the silicon surface by hydrogen; hydrogen renders the surface chemically and it's not reactive. Then by putting the tip on particular places of the sample and scanning, it is possible to modify the surface down to atomic scales.

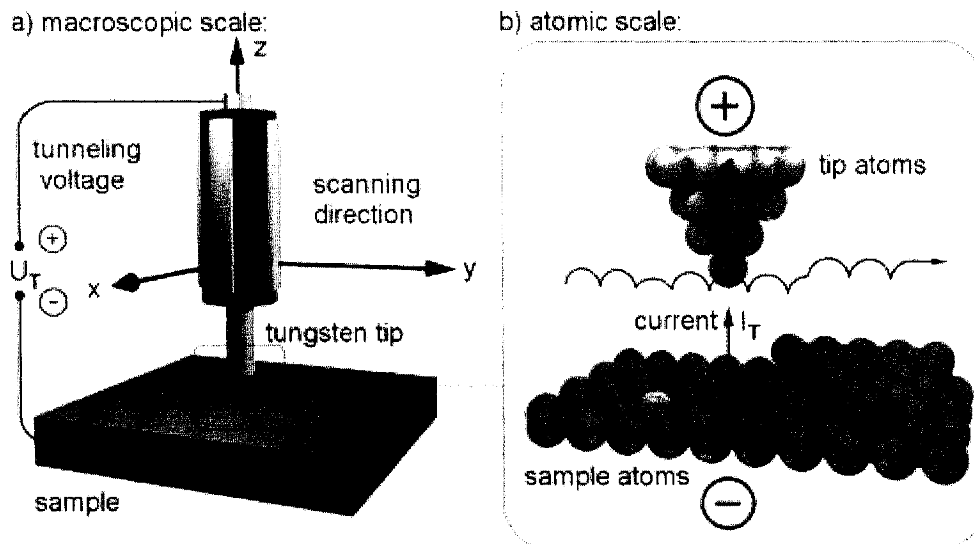

Figure 1-5: Scanning Tunneling Microscope [5]

1.4 Technology Scaling:

In order to continue the technology scaling it is important to go over what has been done in the past that helped us to get to the present stage of technology:

Transistor is the workhorse of the technology scaling. Following the Moore's law, dimensions of transistor has been scaled down by 30% every generation (doubling the transistor density every two years).

The vertical dimension of the transistor has been decreased. As a result of scaling the gate oxide thickness down, we get faster transistors with higher performance.

The supply and threshold voltage has been scaled down by 30% every generation so power became either constant or lower. Looking at the last 30 years of scaling down technology, its performances seems too good to be true .The number of transistors has been doubled every two years and we were able to get up to 15000 MIPS (Millions of Instructions delivered Per Second) of the performance in the last decade.

Transistors have been scaled down well in the past but the question is will they scale down in the future??

Today we are at 90 nm channel length and 2 billion integration capacity .Every two years we have a technology generation so by 2015, 100 billion of transistor integration capacity is expected with in 22nm node and beyond. However the scaling will slow down. Looking at the transistor as a switch, the current flow through the transistor is very limited. When the switch is off, the sub threshold and gate leakage occurs.

1.4.1 Technology Scaling Challenges:

1) Sub-threshold Leakage:

One of the reasons that make following the Moore's law a challenge is the sub threshold leakage. Figure 1-6 shows the sub threshold leakage starting from 0.25 μ technology. As can be seen in the Figure 1-6, for the 0.25 μ technology in 30°C, I_{off} has a negligible value of 1 nA/μ .For the 0.25 micron technology there are about 10 million transistors on a chip and therefore as a whole we have 10 mA/μ leakage ($1\ nA/\mu = 10^{-9}\ A/\mu \times 10^{7} = 10^{-2} A/\mu = 10\ mA/\mu$). So we can conclude that Pentium 2 has a leakage of 10 mA/μ which is not very high. Since then leakage current, $I_{off,}$ has been exponentially increased by 5X in every generation. For the 45 nm technology the leakage will be in the micro ampere range and we can conclude that for one billion transistors in a 45 nm chip we will have thousands amp of leakage which is not reasonable.

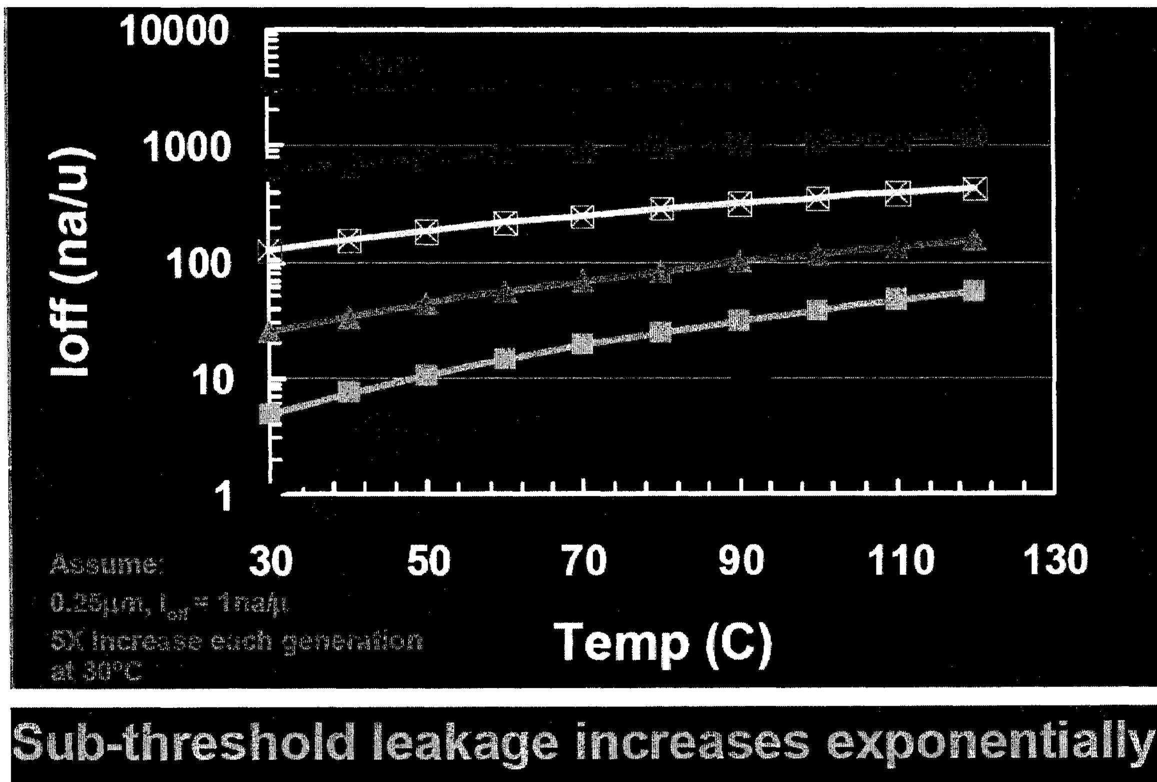

Figure 1-6: Sub-threshold leakage versus temperature, X axis shows the temperature and Y axis shows the off current, I_{off}, the sub-threshold leakage in terms of nA/μ. [2]

2) Gate Leakage:

As can be seen in the Figure 1-7, for a 90 nm MOS transistor the size of the channel is only 50 nm with a 1.2 nm gate dielectric .Because of the thin gate oxide, band to band tunneling occurs through the gate dielectric. This gate leakage doesn't affect the operation because only about 5% of the chip area of a transistor is covered by gate oxide, nevertheless; the problem is that this leakage is a very strong function of supply voltage. Burn-in is a process by which components of a system are exercised prior to being placed in service (and often, prior to the system being completely assembled from those components). ICs' burn-in remains an essential part of the fabrication process.

If we continue the scaling down, it will be impractical to do the burn- in process of the chips because the gate leakage would be very high. In order to decrease the leakage we need a dielectric with higher K (dielectric constant) to replace the gate oxide, maybe potentially a metal instead of the poly silicon. This work is on its way and hopefully we'll see the results in the next few generation.

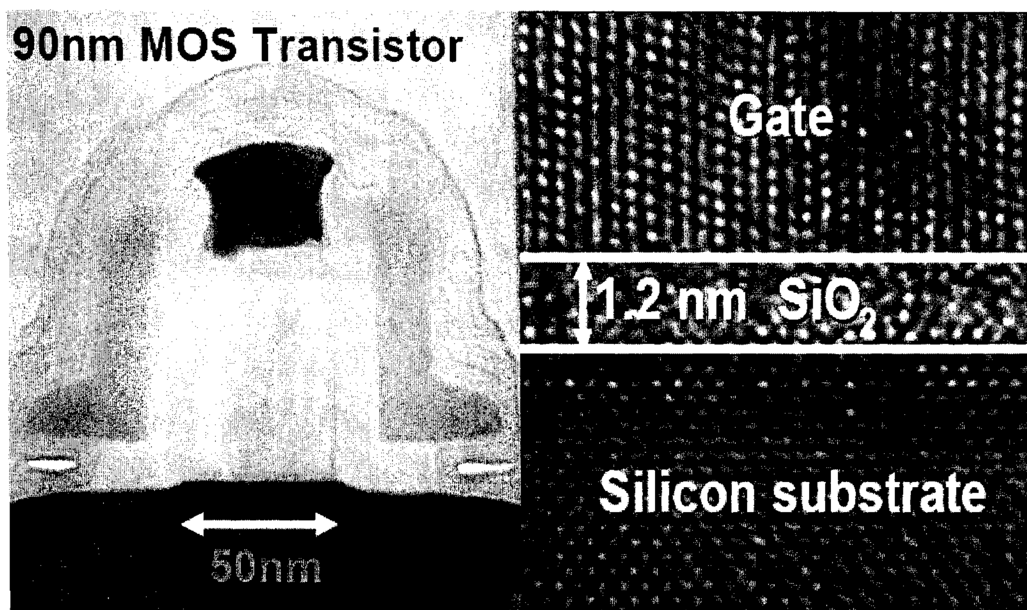

Figure 1-7: For a 90 nm MOS transistor, the channel is only 50 nm with the 1.2 nm gate dielectric. [2]

3) Energy and Power:

By looking at the energy that it takes to do the logic operation versus different technology generation (every two years) diagram we can see that this energy has been scaled down exponentially, see Figure 1-8. With further scaling, because of the gate and sub-threshold leakage, the energy per logic operation scaling will slow down. For example for a 15 mm die, If we start extrapolating from 0.25 micron to the 45 nm generation we can see that 50% leakage occurs .

Figure 1-8 can show us that with this amount high leakage, the way the chips, processors or complex logics have been fabricated is not an option anymore.

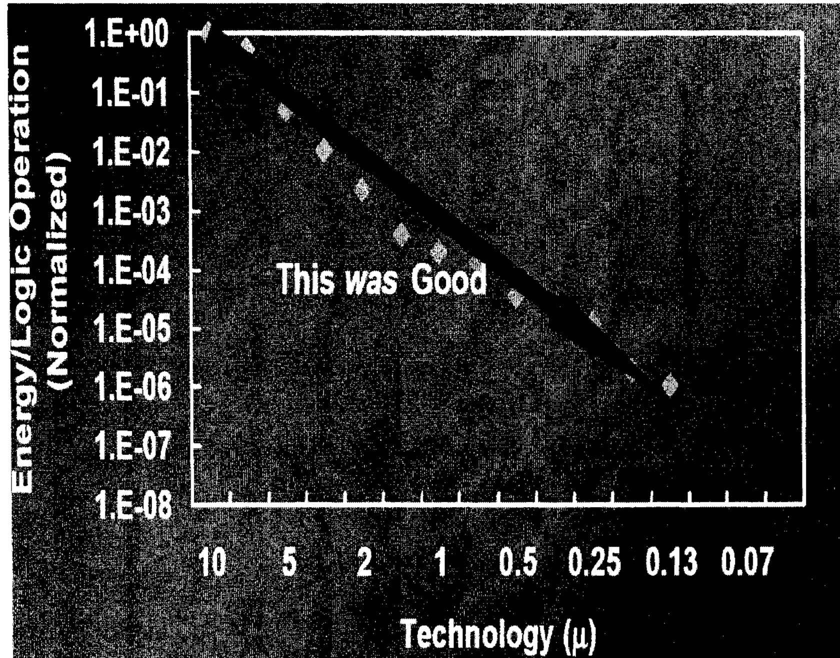

Figure 1-8: The energy to do the logic operation versus the different technology generation (every two years), it can be seen that the energy has been scaled down exponentially. [2]

4) Random doping fluctuation:

The random doping fluctuation will be a challenge and a source of variation for every generation of the transistors. For example, for the 1μ technology the mean number of dopant atoms in the channel is about 1000.Every generation the mean number of dopant atoms decreases .By the time that we reach to 30 nm node, the number of dopant atoms can be approximated around 10 .If we have two transistors side by side the chances that these transistors are going to differ in their characteristics are very high, because it is impossible to have the same number of dopants in each channel. As the size decreases, the transistors characteristics would be more sensitive to the number of dopants.

5) Sub-wavelength Lithography:

As can be seen in Figure 1-9, the light wavelength of 248 nm was used to patent for the 0.25 micron and 180 nm technologies. For 130 nm technology the wave length of about 193 nm was patented.

For further scaling, for example for 32 nm technology, the UV wavelength which is about 13 nm is desirable. In foreseeable future, following the Moore's law, the sub-wavelength lithography should be used. Using the sub wavelength lithography can lead to roughness and line edges and can create static variations in the transistors.

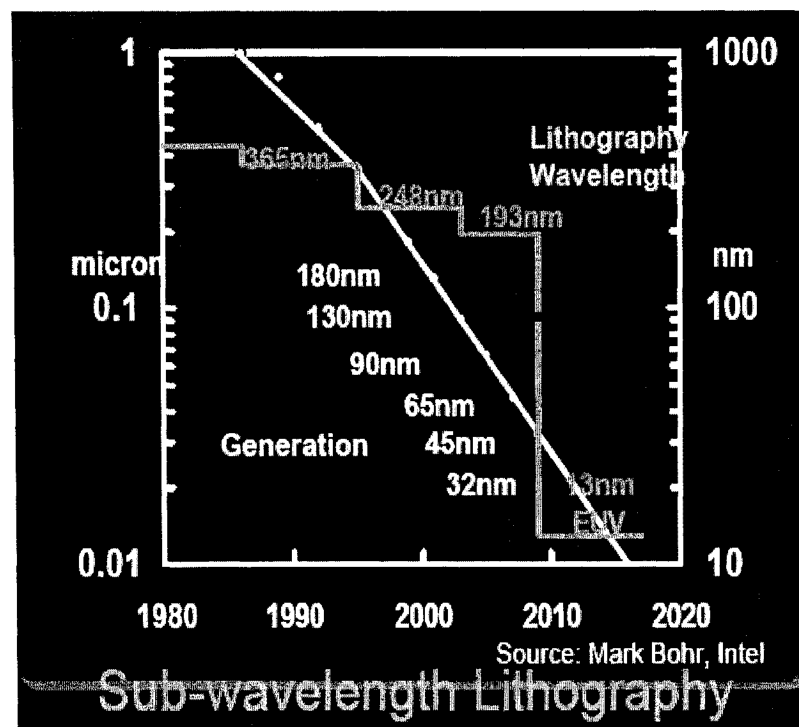

Figure 1-9: Sub-Wavelength Lithography [2]

6) Heat Flux:

There are also dynamics variations, besides statistics variation, in transistors. As can be seen in Figure 1-10, there is a heat flux on Pentium three while it operates. Initially when we start to activate the chip every part of it has the same temperature. In a period of time, there will be different temperature spots on the chip.

The sub-threshold leakage is a very strong function to the temperature. So the leakage variation is going to be all through the chip and therefore power dissipation is going to increase as the number of transistors increase in every generation.

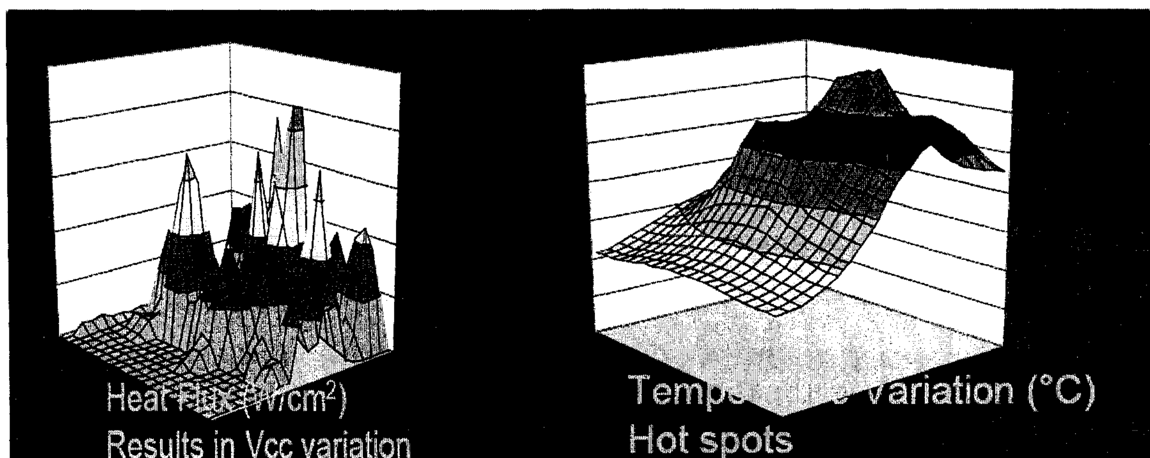

Fig 1-10: Heat Flux and Temperature Variation on the Pentium three chip. [2]

Chapter 2
Carbon Based Materials and Nanotubes

2.1. Carbon Atoms:

Carbon is the sixth element of the periodic table and is listed at the top of column four. Each carbon atom has six electrons which occupy $1s^2$, $2s^2$, and $2p^2$ atomic orbitals. The $1s^2$ orbital contains two strongly bound electrons, and they are called core electrons. Four electrons occupy the $2s^2$ $2p^2$ orbital, and these more weakly bound electrons are called valence electrons.

2.1.1. Hybridization in Carbon Atoms:

Carbon-based materials are unique in many ways. One distinction relates to the many possible configurations of the electronic states of a carbon atom, which is known as the hybridization of atomic orbitals.

In the crystalline phase of carbon atoms the valence electrons give rise to 2s, 2px, 2py, 2pz orbitals which are important in forming covalent bonds in carbon materials. Since the energy difference between the upper 2p energy levels and the lower 2s level in carbon is small compared with the binding energy of the chemical bonds, the electronic wave functions for these four electrons can readily mix with each other, thereby changing the occupation of the 2s and three 2p atomic orbitals so as to enhance the binding energy of the carbon atom with its neighboring atoms. This can be addressed as the reason of the mechanical strength of the carbon materials. This mixing of 2s and 2p atomic orbitals is called hybridization, whereas the mixing of a single 2s electron with n=1, 2, 3 2p electrons is called spn hybridization.

In carbon, three possible hybridizations occur: sp, sp2, and sp3; other group 4 elements such as Si and Ge exhibit primarily sp3 hybridization. Carbon differs from Si and Ge insofar as carbon does not have inner atomic orbitals except for the spherical 1s orbitals and the absence of nearby inner orbitals facilitate hybridization involving only valence s and p orbitals for carbon.

2.2. Carbon Materials:

Carbon materials are found in variety forms such as graphite, diamond, carbon fibers, fullerenes and carbon nanotubes. Carbon has been studied and used for centuries, and carbon science was long thought to be a mature field. Diamond (3D) and graphite (2D) are considered as two natural crystalline forms of pure carbon. So when a whole new class of carbon materials—the fullerenes, such as C60—appeared in the last decade, many scientist were surprised. As a result, we have to change our concept and understanding of long known carbon materials. Carbon has four electrons in its outer valence shell; the ground state configuration is $2s^2\ 2p^2$. In diamond, carbon atoms exhibit sp3 hybridization, in which four bonds are directed toward the corners of a regular tetrahedron. The resulting three-dimensional network is extremely rigid, which is one reason for its hardness. The bond length between sp3 carbons is 1.56Å. Diamond behaves as an insulator because all electrons are localized in the bonds within the sp3 network. In graphite, sp2 hybridization occurs, in which each atom is connected evenly to three carbons in the xy plane, and a weak bond is present in the z axis. The C-C sp2 bond length is 1.42Å. The sp2 set forms the hexagonal lattice. The pz orbital is responsible for a weak Van der Walls bond. The spacing between the carbon layers is 3.35Å. The free electrons in the pz orbital move within this cloud and are no longer local to a single carbon atom (delocalized). This is the reason why graphite can conduct electricity. Table 1.2 classifies different isomers of carbon.

Dimension	0-D	1-D	2-D	3-D
Isomer	C60 fullerene	Nanotube	Graphite fiber	Diamond amorphous
Hybridization	sp2	sp2(sp)	Sp2	Sp3
Bond Length[A]	1.40(C=C) 1.46(C-C)	1.44(C=C)	1.42(C=C) 1.44(C=C)	1.54(C-C)
Electronic Properties	Semiconductor E_g=1.9 ev	Metal or semiconductor	Semimetal	Insulator E_g=5.47 eV

Table 1.2: Carbon is the only material in the periodic table that has isomers from 0 dimensions (0D) to 3 dimensions (3D), as is shown in the table.

2.2.1. Graphite:

Graphite (named by Abraham Gottlob Werner in 1789, from the Greek γραφειν: "to draw/write", for its use in pencils) is, like the diamond, is a polymorph of the element carbon. Graphite is one of the softest mineral known to man which is a good conductor of electricity. Graphite has a sheet like structure where the atoms all lie in a plane and each atom is weakly bonded to the graphite sheets above and below of its plane.

Graphite Sheet

Hexagonal lattice of interacting p orbitals
Weak interactions between layers

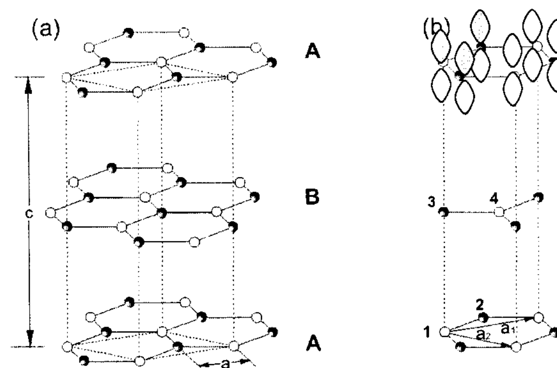

Figure2-1. [6]

Most graphite is produced through the metamorphism of organic materials in rocks. Even coal is occasionally metamorphosed into graphite. Some graphite is found in igneous rocks and also inside of iron. Graphite is flexible but not elastic. It exhibits the properties of a metal and a nonmetal, which makes it suitable for many industrial applications.

The metallic properties include thermal and electrical conductivity. The nonmetallic properties include inertness, high thermal resistance, and lubricity. Some of the major uses of graphite are in high-temperature lubricants, brushes for electrical motors, friction materials, and battery and fuel cells.

2.2.2.Buckyballs:

Buckyballs are the roundest and most symmetrical large molecule known to men. They are a form of Carbon60 which has a unique molecular structure that can be associated with a soccer ball.

C60 is the third major form of pure carbon after graphite and diamond. The structure has 32 faces, in which 12 of them are pentagons and 20 are hexagons. It has a hybridized carbon atom located at all 60 of the vertices of the molecule. Buckyball is the only molecule composed of a single element to form a hollow spheroid. When buckyballs are compressed to 70 percent of its original size, they become more than twice as hard as diamonds.

The formal name for the molecule's structure is truncated icosahedrons. Carbon 60 is not the only form of buckyball. They can form into clusters exceeding 100 carbon atoms. However, when more atoms are added to the buckyball, it loses its perfect symmetry and becomes egg-shaped. The symmetry of the carbon 60 makes it the most stable form of the Buckyball.

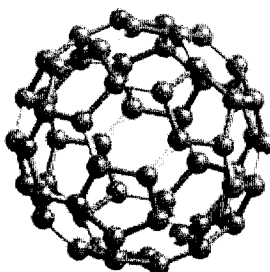

2.2.3. Carbon Nanotubes (CNT):

Carbon nanotubes are fullerene-related structures that consist of graphene cylinders that are closed at either end with caps containing pentagonal rings. They were discovered in 1991 by the Japanese electron microscopist Sumio Iijima who was studying the material deposited on the cathode during the arc-evaporation synthesis of fullerenes. He found that the central core of the cathodic deposit contained a variety of closed graphitic structures including nanoparticles and nanotubes, of a type which had never previously been observed. Since the pioneering work of Iijima, the study of carbon nanotubes has progressed rapidly.

Some time later, Thomas Ebbesen and Pulickel Ajayan, from Iijima's lab, showed how nanotubes could be produced in bulk quantities by varying the arc-evaporation conditions. This paved the way to an explosion of research into the physical and chemical properties of carbon nanotubes in laboratories all over the world. One of these properties is that nanotubes can behave as quantum wires. They also exhibit interesting mechanical properties like high tensile strength and good flexibility. They also have very high thermal conductivity and almost zero in-plane thermal expansion. The carbon-carbon chemical bonding as well as their tiny structure is believed to be responsible for their very unique properties. A carbon nanotube is a tubular form of carbon with a diameter as small as 1 nm. The diameter can change from 0.7 nm to 2nm. The length can be from few nanometers to several microns. Carbon nanotubes are only made of carbon atoms.

To understand the CNT's structure, it helps to imagine folding a two dimensional graphene sheet and assume that hybridization is not altered after folding it. Depending on the dimensions of the sheet and the way it is folded, several variations of nanotubes can arise. Because of the single or multilayer nature of graphene the resulting tubes can be single or multi wall type.

Generally speaking, there are two types of CNTs: single-wall carbon nanotubes (SWNTs) and multi-wall carbon nanotubes (MWNTs). As their names imply, SWNTs consist of a single, cylindrical graphene layer, where as MWNTs consist of multiple graphene layers telescoped about one another.

A variety of tubes-based on the orientation of the benzene rings on the graphene tubes-are possible. If the orientation is parallel to the tube axis, then the resulting "zigzag"

tubes are semiconductors. Single-Wall carbon nanotubes (SWNT) are two dimensional graphene sheets rolled into nanometer diameter cylinders that can be either 1D metal or semiconductor. With the appropriate chirality's, SWNT can be semiconducting, with a bandage reversely proportional to the diameter of the tube.

2.3 Structure of Single-Wall Carbon nanotubes:

A single–wall carbon nanotube can be described as a graphene sheet rolled into a cylindrical shape so that the structure becomes one dimensional with axial symmetry, and in general exhibiting a spiral conformation, called chirality. The chirality is given by a single vector called the chiral vector which is shown by C_h.

The structure of carbon nanotubes has been explored early on by high resolution Transmission Electron Microscopy (TEM) and Scanning Tunneling Microscopy (STM) techniques, resulting in understanding that nanotubes are seamless cylinders derived from the honeycomb lattice. Carbon nanotubes are representing a single atomic layer of crystalline graphite, called a graphene sheet. The unit cell of the 1D carbon nanotube is the rectangle OAB'B, see Figure 2-2, defined by the vectors C_h and T.

Vectors a_1 and a_2 are the unit vectors that define the area of the unit cell of the 2D graphene, see Figure 2-2. They can be written in the xy coordination as follow:

$$a_1 = \sqrt{\frac{3}{2}} a\hat{i} + \frac{1}{2}\hat{j} \quad \text{and} \quad a_2 = \frac{\sqrt{3}}{2} a\hat{i} - \frac{1}{2}\hat{j} .$$

It should be noted here that a_1 and a_2 are not orthogonal to each other.

The structure of a single-wall carbon nanotube is specified by the vector OA in Figure 2-2 which corresponds to a section of the nanotube perpendicular to the nanotube axis.

The transitional vector T is defined to be the unit vector of a 1D carbon nanotube. Vector T is parallel to the nanotube axis and is normal to the chiral vector C_h in the unrolled honeycomb lattice. The lattice T shown as OB in Figure 2-2 can be expressed in terms of the basis vectors a_1 and a_2 as: $T=t_1a_1+t_2a_2$.This vector corresponds to the first lattice point of the 2D graphite sheet through which victor OB passes.

The Chiral angle is between the chiral vector and the zigzag direction as can be seen in Figure 2-2 and it can be written as:

$$\theta = \tan^{-1}[\sqrt{3}n/(2m+n)] \qquad (2.1)$$

From the equation (2.1), we can see that the chiral angle is θ=30° for the (n,n) armchair nanotube and it would be θ=60° for (n,0) zigzag nanotube.

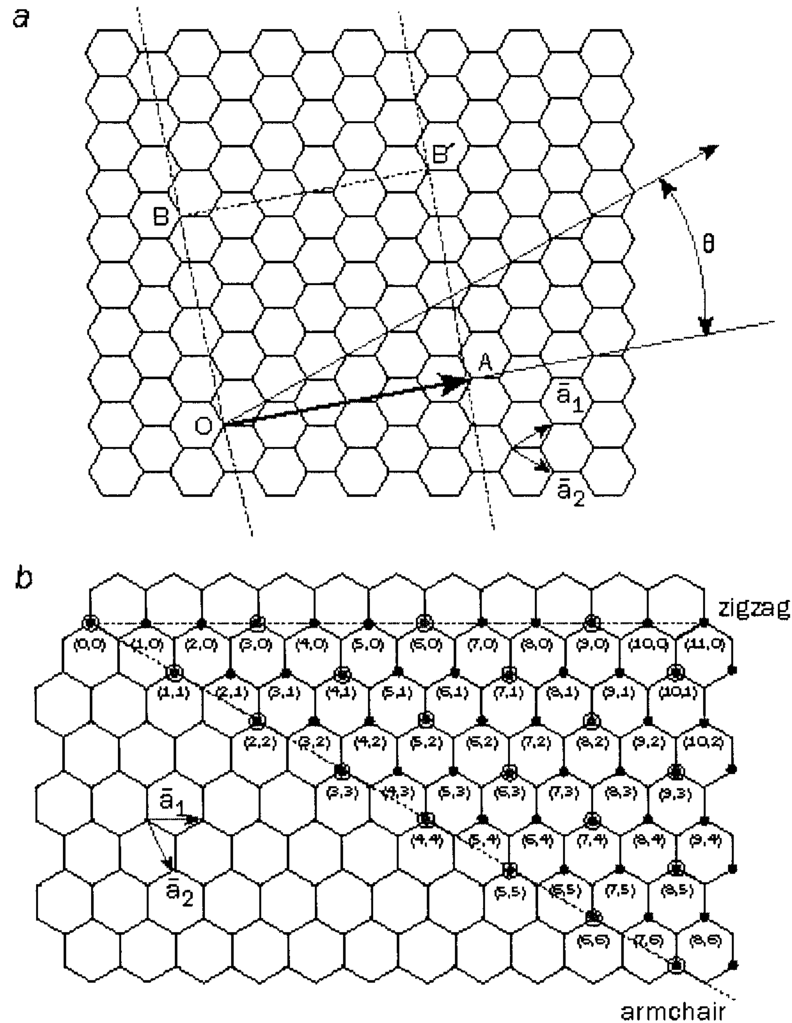

Figure 2-2: The unrolled honeycomb lattice of a nanotube. [8]

The circumference of any carbon nanotube is expressed in terms of the chiral vector $C_h=na_1+ma_2$, (n, m are integers, 0<<m<<n).The construction of the carbon nanotube depends uniquely on the pair of integers (n,m) which specify the chiral vector. In the (n, m) notation for $C_h=na_1+ma_2$, the vectors (n, 0) or (0, m) denote zigzag nanotubes and (n, n) is the notation for armchair nanotubes. All other vectors (n, m) correspond to chiral nanotubes.

2.3.1 Classification of carbon nanotubes:

Theoretical calculations have shown that the electronic properties of the carbon nanotubes are very sensitive to their geometric structure. Although graphene is a zero–gap semiconductor, theory has predicted that carbon nanotubes can be metals or semiconductors with different energy gaps, depending very sensitively on the diameter and helicity of the tube, i.e., on the indices (n,m).

Three distinct types of nanotube structures can be generated by rolling up the graphene sheet into a cylinder, see Table 1.2 .The zigzag and armchair nanotubes, respectively, correspond to chiral angles of $\theta=0$ and, 30° , and chiral nanotubes correspond to $0<\theta<30°$.

Type	θ	C_h
Armchair	30	(n,n)
Zigzag	0	(n,0)
Chiral	$0<\theta<30$	(n,m)

Table1.2: The classification of carbon nanotubes.

The physics behind this sensitivity of the electronic properties of carbon nanotubes to their structure can be understood within the band-folding picture. It is due to the unique band structure of graphene sheet, which contains the energy states crossing the Fermi level at only two not equivalent points in k-space, and to the quantization of the electron wave vector along the circumferential direction. An isolated sheet of graphite is a zero-gap semiconductor which its electronic structure near the Fermi energy is given by an occupied π band and an empty π^* band. These two bands meet at the Fermi level at the

K points in the brillouine zone. The electronic structure of carbon nanotube is derived by a simple tight-binding calculation for the pi-electrons of carbon atoms. The electronic structure of a single-wall nanotube can be obtained simply from that of two –dimensional graphite.

The remarkable electrical properties of SWNTs stem from the unusual electronic structure of the two –dimensional material, graphene, from which they are constructed.

Graphene-a single atomic layer of graphite-consists of a 2-D honeycomb structure of sp2 bonded carbon atoms. Its band structure is quite unusual; it has conducting sates at the Fermi level, E_F, but only at specific points at the corners of the first Brillouine zone and along certain directions in momentum space. It is called a zero-bandgap semiconductor since it is metallic in some directions and semiconducting in the others. In an SWNT, the momentum of the electrons moving around the circumference of the tube is quantized, reducing the available states to slices through the 2-D band structure.

As can be seen in the Figure 2-3, the Fermi surface of an ideal graphite sheet consists of the six corner K points. When forming a tube, owing to the periodic boundary conditions imposed in the circumferential direction, only a certain set of k states of the planar graphite sheet is allowed.

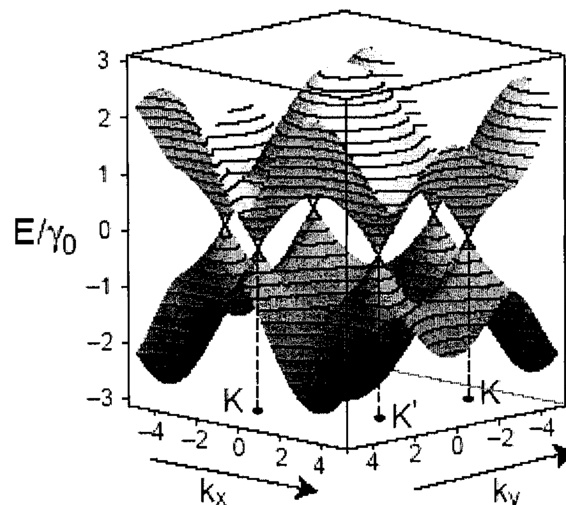

Figure 2-3: Band structure of graphene. [7]

The allowed set of k depends on the diameter and helicity of the tube. Whenever the allowed k's include the point K, the system is a metal with a nonzero density of state at the Fermi level.

The general rules for the single-walled carbon nanotubes are as followed:

- (n, n) tubes are metals.
- (n, m) tubes with n-m=3j, where j is a nonzero integer, are very tiny-gap semiconductors
- All other carbon nanotubes are large gap semiconductors.

Strictly within the band-folding scheme, the n-m=3j tubes would all be metals, but because of the tube curvature effects, a tiny gap opens for the case where j is nonzero. Hence, carbon nanotubes come in three varieties: large-gap, tiny-gap, and zero- gap. The (n, n) tubes, also known as armchair tubes, are always metallic within the single – electron picture, being independent of curvature because of their symmetry. As the tube radius R increases, the band gaps of the large-gap and tiny-gap carbon nanotubes decrease respectively with 1/R and $1/R^2$ dependence. Thus, for most practical purposes, all the n-m=3j tubes can be considered as metallic at room temperature.
In short, calculations revealed that nanotubes could be either metallic or semiconducting, depending on their helicity and diameter. The armchairs tubes are always metallic, whereas the zigzag and chiral tubes can be either metallic or semiconducting.
The terminations of each of the three different nanotubes are shown in Figure 2-4. The terminations are often called caps or end caps and they consist of a "hemisphere" of a fullerene. Each cap contains six pentagons and an appropriate number and placement of hexagons that are selected to fit perfectly to the long cylindrical section.

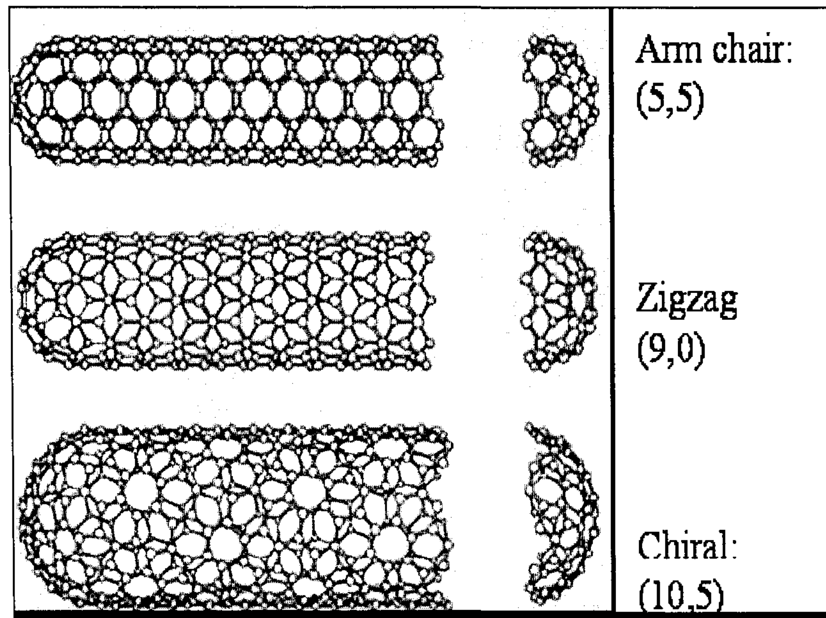

Figure 2-4: Carbon nanotube cylinders with different chiralities. [8]

The diameter of the carbon nanotube, d_t, is given by L/π, in which L is the circumferential length of the carbon nanotube and it can be calculated as:

$$d_t = \frac{L}{\pi}, L = |C_h| = \sqrt{C_h.C_h} = a\sqrt{n^2 + m^2 + nm}$$

Because electrons are confined in the radial directions of the singular plane of the graphene sheet, electronic conduction process in nanotube is quantum confined.

The conduction occurs in armchair (metallic) tubes through gapless modes because the valence and conduction bands always cross each other at Fermi energy for a certain special wave vector (corresponding to the K point in the Brillouine zone).

In most of the chiral tubes, where the unit cell contains a large number of atoms, the one-dimensional band shows an opening of the gap at Fermi level and therefore has semiconducting properties.

In certain cases, however, zigzag and chiral tubes also become conducting when one of the sub bands still crosses one of the K points. The energy gap for a semiconductor

nanotube, which is inversely proportional to its diameter, can be directly observed by scanning tunneling microscopy measurements. When the diameter of the tube increases, the band gap (which varies inversely with the tube diameter) tends to zero, yielding a zero gap semiconductor that is essentially equivalent to the planar graphene sheet.

In a MWNT, the electronic structure of the smallest inner tube is superimposed by several outer, larger planar graphene like tubes. Thus it can be assumed that any measurement on the electronic properties of MWNTs is going to result in semi metallic behavior like the parent graphite structure.

2.3.2. Synthesis of Carbon Nanotubes:

The first experimental identification in 1991 of carbon nanotubes was on multiwall nanotubes. The experimental discovery of single-wall carbon nanotubes in 1993 further stimulated work in the field; although at first only small quantities of single-wall nanotubes were available experimentally for systematic studies.

Carbon nanotubes were first noticed at the ends of graphite electrodes that were used in an electric arc discharge employed in fullerene synthesis.

Typically the deposit builds up on the cathode surface from evaporated anode during an arc struck between pure graphite electrodes in 500-torr helium pressure at 20 V and 50-100 A. SWCNTs are more difficult to grow.

Single-Wall Nanotube Synthesis:

There are three methods which are currently used to produce mass quantities of SWCNT; arc-discharge, chemical vapor deposition (CVD), and laser ablation.

However, none of the three methods are ideal for electronic industry and none of them can control the properties of the nanotube. They all produce mixtures of metallic and semiconducting nanotubes with a wide different range in CNT lengths and diameters. Below is a description of each process that creates carbon nanotubes.

-Laser Vaporization Synthesis Method

In 1996, R.Smalley was able to produce nanotubes by pulsed YAG laser ablation of graphite target in a furnace at 1200°C. [18]

An efficient way for the synthesis of bundles of single-wall carbon nanotubes with a narrow diameter distribution employs the laser vaporization of a graphite target.

In the early reports of the laser synthesis technique, high yields with 70%-90% conversion of graphite to single-wall nanotubes were reported in the condensing vapor of the heated flow tube (operating at 1200°C).A CoNi/graphite composite laser vaporization target was used, consisting of 1.2 atom %Co-Ni alloy with equal amounts of Co and Ni added to the graphite (98.8 atom%).[16]

Two sequenced laser pulses were used to evaporate a target containing carbon mixed with a small amount of transition metal from the target. Flowing argon gas sweeps the entrained nanotubes from the high temperature zone to the water cooled copper collector downstream, just outside the furnace. A detailed transmission electron microscopy study of carbon nanotubes prepared by the laser vaporization method has shown that the carbon nanotube chiral indices (n,m) are mainly (10,10)(~44%), (9,9)(~20%), and some (12,8)

X-ray diffraction (which views many ropes at once) and transmission electron microscopy experiments (which view a single rope) show that the diameter of the single-wall nanotubes have a strong peaked distribution at 1.38_+0.02 nm diameter, very close to the diameter of an ideal (10,10) nanotube.

-Arc-Discharge Method of Synthesizing Carbon Nanotubes

Nanotubes were first found in soot produced in arc discharge with catalyst metals such as Fe, Ni and Co by S.Iijima in 1991.The carbon arc provides a simple and traditional tool for generating the high temperatures needle for the vaporization of carbon atoms into a plasma(>3000°C).

In this process, two graphite rods are placed millimeters apart and are attached to a power supply. At the moment that power supply is turned on, a spark vaporizes the carbon into plasma; when the plasma re-condenses, approximately 30% of it forms nanotubes at catalyst sites. [16] [17]

Once the arc is in operation, carbon deposit forms on the negative electrode. As the carbon nanotubes form, the length of the positive electrode (anode) decreases.

Arc-discharge, see Figure 2-5, has been developed into an excellent method for producing both high quality multi-walled nanotubes and single-wall nanotubes. The synthesized nanotubes usually have lengths in the order of ten microns and diameters in the range of 5-30 nm.The produced nanotubes are usually attached together and form a bundle by strong Van der Walles interactions.The by-product of the arc-discharge is multi –layered graphite.

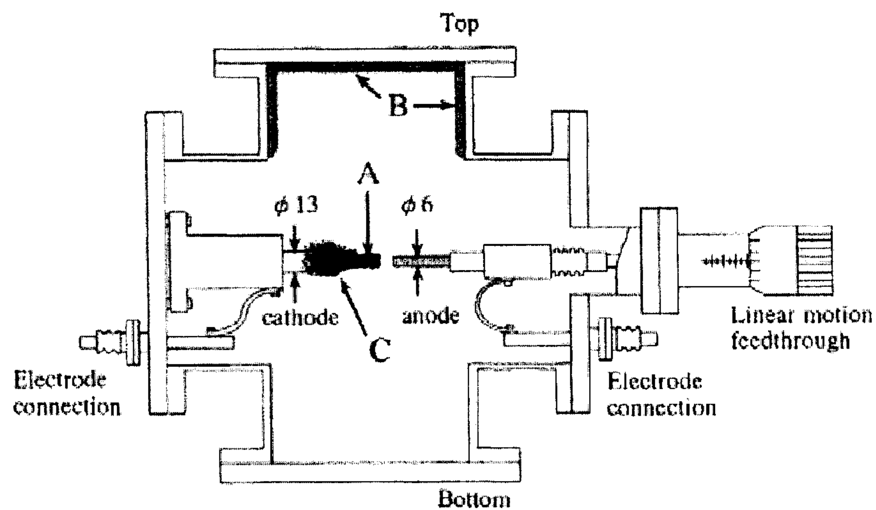

Figure 2-5: A schematic diagram of the arc-electric discharge method as was developed by Saito in 1995. [9]

Both methods, Laser Vaporization Synthesis and Arc-Discharge, are difficult to integrate because the location and alignment of the synthesized nanotubes can not be controlled.

-Vapor Growth Method:

The CVD method can theoretically produce large quantities of nanotubes at site specific locations. [23] This process involves the decomposition of hydrocarbons (e.g. methane, benzene, acetylene, naphthalene, ethylene, etc) over metal catalysts (e.g. Co, Ni, Fe, Pt, Pd) that are deposited at predefined locations on a substrate. The gas flow direction and the catalyst placement, by e-beam lithography, are closely monitored to help align nanotubes carefully on the substrate. The metal catalyst is placed in a heating chamber at approximately 600°C and hydrocarbon gas, such as methane, is added to the heating chamber.

The gas decomposes and frees carbon atoms; these free carbon atoms can recombine at either a catalyst site or at the end of a carbon nanotube to increase the length of the nanotubes

Chapter 3
Carbon Nanotubes Applications

Most applications of the nanotubes are based on its unique electronic structure, mechanical strength, flexibility and dimensions of nanotubes.

3.1 Mechanical Applications

C=C bond in graphite is the strongest bond in nature; a carbon nanotube is widely regarded as the ultimate fiber with regard to its strength in the direction of the nanotube axis. Covalent bonds are one of the strongest in nature; a structure based on a perfect arrangement of these bonds oriented along the axis of nanotubes would produce an exceedingly strong material.

Nanotubes come close to being the best fiber that can be made from graphite structure.

A carbon fiber however, consists of many graphite planes and microscopically exhibits electronic properties that are predominantly two-dimensional.

Just as for the carbon fibers that are produced commercially for aerospace applications, carbon nanotube show excellent strength characteristics under extension, and molecular dynamics simulations indicate that an increase in length of several percent without fracture might be possible.

In addition single-wall nanotubes show remarkable flexibility, and can be bent round small circles or bout sharp bends without breaking. Carbon fibers fracture easily under compression but carbon nanotubes form ridges under compression which can relax elastically when the stress is released.

Due to high mechanical strength and elasticity nanotubes can be used as nanoprobes; for example as tips of scanning probe microscopes. This idea has been demonstrated successfully and a nanotube tip on an atomic force microscope was used to image the topography of TiN-coated aluminum film.

3.2. Electronics Applications:

Since the beginning of the last decade carbon nanotubes have received remarkable attention from the scientists since it has been found that they possess unique electronic properties. This makes nanotubes suitable for applications in microelectronics and nanoelectronics like diodes, transistors and displays.

Most of the electronics application today is based on single nanotubes whereas there has not been any preference between single wall and multi wall nanotube in its other applications.

By far, using nanotubes as quantum wires has received most of the attention. The single wall nanotube field effect transistor which operates at room temperature consists of a nanotube bridging two metal electrodes. The band structure suggested for this device is the same as the one suggested for similar semiconducting devices. The performance in terms of switching speeds is comparable to existing devices.

Another application is the use of the nanotube as electron emitters. The film of aligned tubes is transferred onto a substrate and a voltage is applied across the supporting film and collector. Such nanotube films act like field emission sources with turn-on voltages of a few tens of volts and electron emission at current densities of a few hundred milli amperes per centimeter squared. The nanotube electron source remains stable over several hours of field emission. Obtaining uniformly aligned tubes is still an issue which is essential for getting uniform emission.

Due to the conducting nature of the tubes they can also be used as STM tips.

3.3 Advantages of using Carbon Nanotubes over Silicon Wires:

Based on the assumption that all the technological problems are solved, there are some potential benefits to use carbon nanotubes over silicon wires, some of them are listed as:

1. Chemical synthesis controls the key dimensions. The key nanometer radius size is produced during the growth fabrication of the nanotube like using the laser ablation technique or CVD which is different from fabricating silicon through etching method.

2. Charge transport is one-dimensional and backscattering is strongly suppressed because of the limited states available which can be resulting in high "mobility" of electrons/holes and consequently high I_{on} in a carbon nanotube field effect transistor.

3. The off state of the transistor is expected to be very good in carbon nanotube field effect transistor. One of the strengths in miniaturization of today's MOSFET technology is that by going to the thinner silicon structures we can get a better desirable electrostatics. Whereas in nanotubes, we already have a very thin body and the smallness of its diameter (it can be around 1 nm) can result to a good electrostatic control of the gate and consequently a very good off state as well as the good on state.

4. Electron and hole transport are equal (same m*) which means that n-type and p-type CNFETs can be identical. For CMOS technology it is desirable to have n-type as well as p-type to build a complimentary CMOS .For Carbon nanotube the dispersion looks the same for electrons in the conduction band as well as the holes in the valence band and accordingly the effective mass is similar. According to the dispersion relation one can hope to see n-type and p-type transistors behave the same and give us the same performance.

5. All chemical bonds are satisfied and therefore dielectrics other than SiO_2 can be used in the field effect transistor. All the carbon atoms in hexagonal arrangements are happy with their nearest neighbors and the carbon nanotube configuration does not show any

dangling bonds. Comparing this situation with silicon, introducing the dielectric to the silicon crystal can break the symmetry of silicon and it can give rise to a problem of combination of silicon with other dielectrics other than silicon dioxide. On the other hand, because of the absent of dangling bonds on the surface of the nanotubes, they can be combined with various dielectrics other than SiO_2 and it can lead to the flexibility of having higher dielectric constant(K) in transistors.

6. By going to the thinner body in silicon wires the mobility degrades .On the other hand the conduction in nanotubes is happening on the carbon nanotube surface and is ballistic.

7. The strong confinement around the circumference leads to a large spacing between 1D subbands (~1 eV for a ~1 nm tube in contrast to ~10meV for typical semiconductor wires), which means that the 1D nature is retained up to room temperature and well above.

8. As we know silicon can only be semiconducting; on the other hand, carbon nanotubes can be metallic as well as semiconducting and therefore all nanotube based electronics may become possible. There is no control to make a specific type but still it is encouraging to think about metal nanotubes acting as interconnects in the future integrated circuits and semiconducting nanotubes can act as the active devices. For transistor's applications semiconductor nanotubes are needed.

3.3.1 Selecting Semiconducting Tubes:

The semiconducting properties of Carbon nanotubes are desirable for its transistor's application. There is a method called constructive destruction which is used to get rid of metallic tubes in the bundles of carbon tubes that are consist of both semiconducting and metallic carbon nanotubes. By attaching contacts to the two ends of the bundles of tubes - source and drain-and then biasing the side gate in a way that semiconducting tubes are kept in the off states, at some point metallic tubes break, see Figure 3-1, and the remaining semiconducting carbon nanotubes that that are survived during this process can be used for fabrication of field effect transistors.

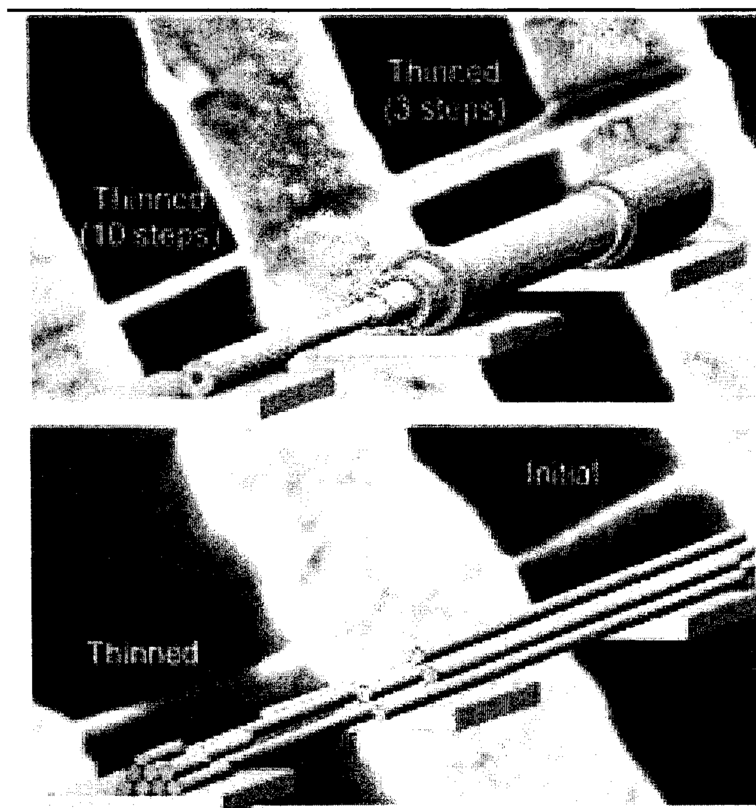

Figure 3-1: The process of selecting semiconducting tubes out of multi walled carbon nanotubes are shown at the top and the process of selecting semiconducting tubes out of single walled carbon nanotubes is shown in the second picture. [10]

Chapter 4
Carbon Nanotube Field Effect Transistor (CNFET)

4.1. Transistor based on a single carbon nanotube:

With the scaling limit of conventional transistor in sight, there is a rapidly growing interest in nanowire transistors with one dimensional (1-D) channels, such as carbon nanotube transistors, and silicon nanowire transistors.

Due to the 1-D channel geometry, the electrostatics of nanowire devices can be quite different from bulk semiconductor devices. While metallic nanotubes can play a role of interconnects in future electronic circuits, their semiconducting counterparts can be used as the basic elements of transistors like the field effect transistor with semiconducting single wall nano tube as the channel operating at room temperature. Although carbon nanotube FETs (CNFETs) with significantly better device performance significantly than silicon MOSFETS have recently been reported, CNFET technology is still at an early stage.

Despite the similarity of CNFET to the conventional devices, there is now ample evidence that CNFETs generally operate by an entirely different principal. Device structures are still primitive and device physics is still relatively unexplored. The carbon nanotube is one dimensional, which greatly reduces the scattering probability. As a result the device operates in the ballistic regime. The nanotube conducts essentially on its surface where all the chemical bonds are saturated and stable. There are no dangling bonds on the surface of the carbon nanotube, so there is no equivalent of the silicon/silicon dioxide interface and there is no need for careful passivation of the interface between the nanotube channel and the gate dielectric. The Schottky barrier at the metal –nanotube contact is the active switching element in an intrinsic nanotube transistor.

One of the possible types of CNFETs is a Schottky barrier FETS which require careful alignment of the Schottky barrier and the gate electrode, which may be a manufacturing challenge. Charge density of the tube varies with the contact and insulator properties. At the metal-semiconductor contact there is a Schottky barrier (SB), i.e. an energy barrier for carrier transport, which can be a sever limitation for devices. In silicon semiconductor devices this problem is generally avoided by replacing metal contacts with heavily doped regions of the semiconductor. However, nanotube devices have generally relied on direct metal-semiconductor contacts.

4.2 Schottky Barrier Field Effect Transistors:

4.2.1 Fabrication

The source and drain region is made of silicide or metal rather than heavily doped semiconductor .From a fabrication point of view, SBCNFETs require no ultrahigh doping in source /drain region, and the metal-semiconductor junctions between source/drain and channel can be abrupt. Nonetheless, good device performance can be obtained. The reason is that the Schottky barrier represents a much less sever limitation for CNFETs than for conventional FETs, due to the quasi-one-dimensional (1D) geometry. Operation is controlled by the electric field from the gate which can lead to strong band bending allowing carriers to tunnel though the interfaces. To use nanotubes in future circuits it is essential to be able to make transistors from them. IBM reported that they have successfully fabricated and tested nanotube transistors using individual multi-wall or single-wall nanotubes as the channel of a field-effect transistor (FET) ,see Figure4-1 and Figure 4-2, on SiO_2 substrate using gold as source and drain.

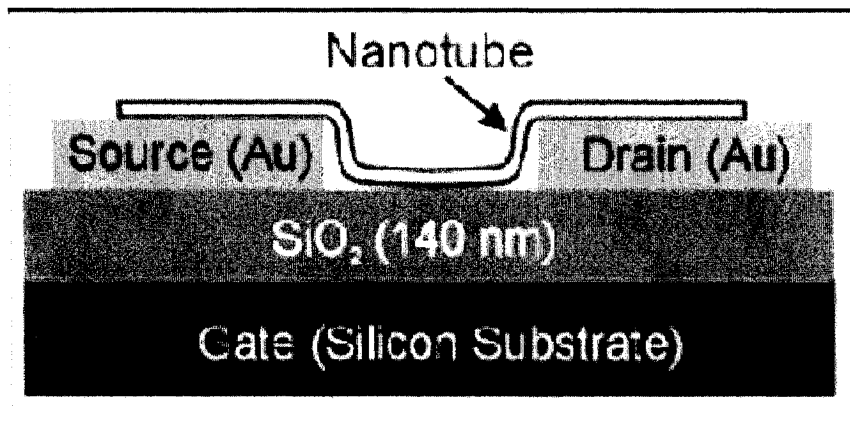

Figure 4-1: Carbon nanotube transistor on SiO_2 substrate using gold as source and drain [11].

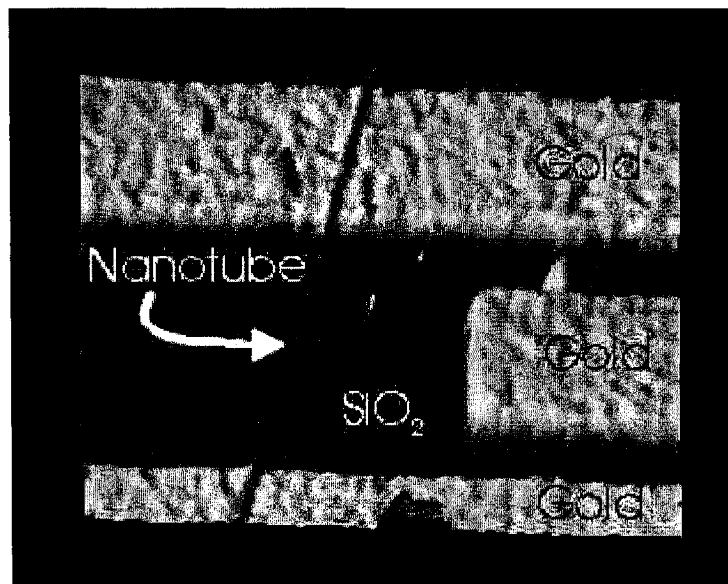

Figure 4-2: Top view of a CNFET with SiO_2 substrate and gold source and drain [11].

The gate was located underneath the tube, separated by an insulator. A problem with this design was that the tube was exposed to the air and hence due to a property of the tube it could operate only as a p-type transistor. Carbon nanotubes are naturally act as p-type devices when they are exposed to air. The reason is that oxygen in air causes the Fermi level at the contacts shift closer to the valence band. These devices displayed gate voltage modulation of the drain current over several orders of magnitude. Due to the thick gate dielectric, these devices required large values of gate voltage (several Volts) to turn on, which make them unattractive for practical applications. Since then, it has been improvements and advances in CNFET electrical characteristics and structures. The carbon nanotubes were deposited on the substrate and the electrodes were patterned on top of the CNTs rather than laying the nanotubes over source and drain electrodes, see Figure 4-3. This way the metal/nanotube weak Van der Walls forces for contacts could be improved .This way other metals rather than Au could be used to replace the electrodes like Ti and Co and Pd .This modification resulted in significant reduction in the contact resistance and the better Fermi level alignment relative to the nanotube band edge.

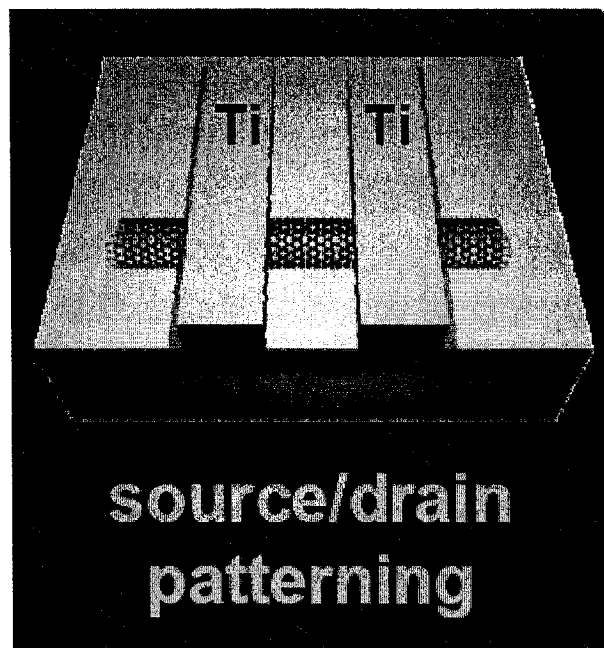

Figure 4-3: Source/drain patterns on top of the carbon nanotube. [2]

Top Gated Carbon Nanotube Field Effect transistor: Fabrication

Further, in order to improve the function of CNFET, another fabrication design was introduced, the top gated field effect transistors, see Figure 4-4.

To fabricate them first carbon nanotubes are grown on top of the silicon/silicon dioxide substrate. Through lithography, metal contacts, commonly made of Titanium or Cobalt, are placed over the nanotube to create source and drain contacts.

In order to form a strong interaction between the metal and the nanotube the system is annealed at 850°C for about 100 seconds to form metal carbide. The carbon nanotube structure can withstand temperatures up to its melting point which is around 3,000°C. [16]. Then by depositing LTO (low temperature silicon dioxide) on top of the structure the gate dielectric film is formed .By defining titanium or aluminum metal gate right between source and drain the electrostatics in the device can be controlled.

With this approach the voltage is tuned down to about Volt ranges. As can be seen in Figure4-4, this structure resembles the MOSFET but here nanotube is the channel for conduction.

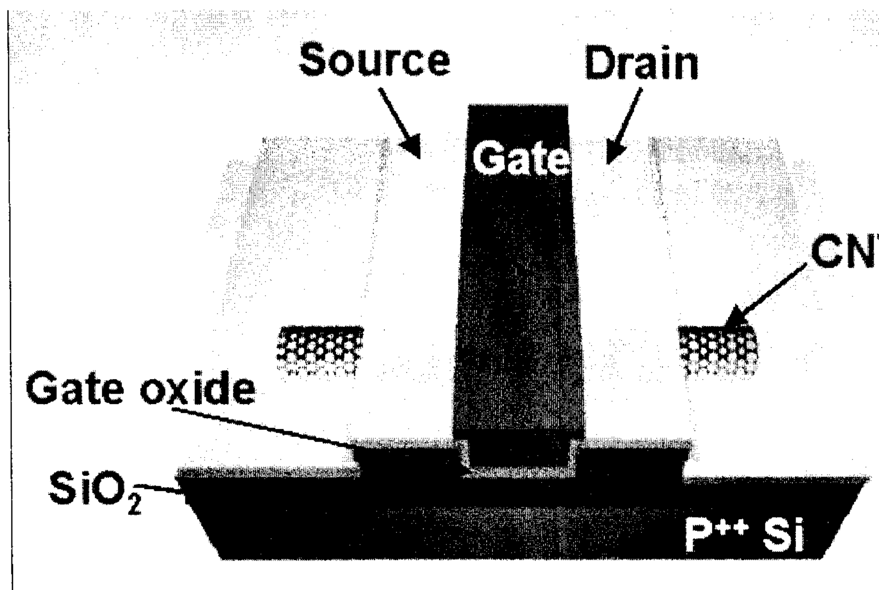

Figure 4-4: Top gated CNFET. [2]

4.2.2 Schottky Barrier Field Effect Transistors: Operation

There is a strong belief that the Schottky barrier at the carbon nanotube and metal contact is the dominant factor in the operation of carbon nanotube field effect transistors. As will be discussed more in this chapter; the bonding of a CNT to a metal electrode results in charge transfer and creation of the Schottky barrier at the CNT/metal interface. That's why the energy band line and charge transfer is strongly affected by the absorption of species such as gaseous oxygen at the junction. Within the framework of the Schottky barrier model of conduction the effect of ambient air on the performance of CNFETs can be understood.

The original back gated CNFETs operating in air function as a p-type transistor without any doping of the carbon nanotube. The reason is that the absorbent oxygen changes the surface potential because it changes the local work function of metal/CNT interface. Oxygen lifts the Fermi level of the nanotube towards the valence band that's why hole injection takes place.

On the other hand, the characterization of the nanotube changes from p-type to n-type if the transistor is moved from air to vacuum. In the annealing process, absorbed oxygen is driven away from the contacts which result to the shifting of the Fermi level up to the conduction band. In return, electron conduction increases at the device and the transistor would have better n-type characteristic. In short CNTs are p-type in the oxygen ambient and n-type or intrinsic in vacuum. So physically, annealing removes the oxygen from the contacts, which changes the surface potential of the metal contacts to the CNT band gap. This process is reversible; if the CNT is exposed to air, the original IV characteristics will return and the situation changes where the nanotubes become converted from n-type to p-type.

In Figure 4-5, Au-contacted p-FET is converted to n-FET by annealing in vacuum. Then as denoted by arrows, slow reintroduction of oxygen simultaneously suppresses electron conduction at positive V_{gs} and increases the hole conduction at negative V_{gs} without changing the threshold voltage of the transistor.

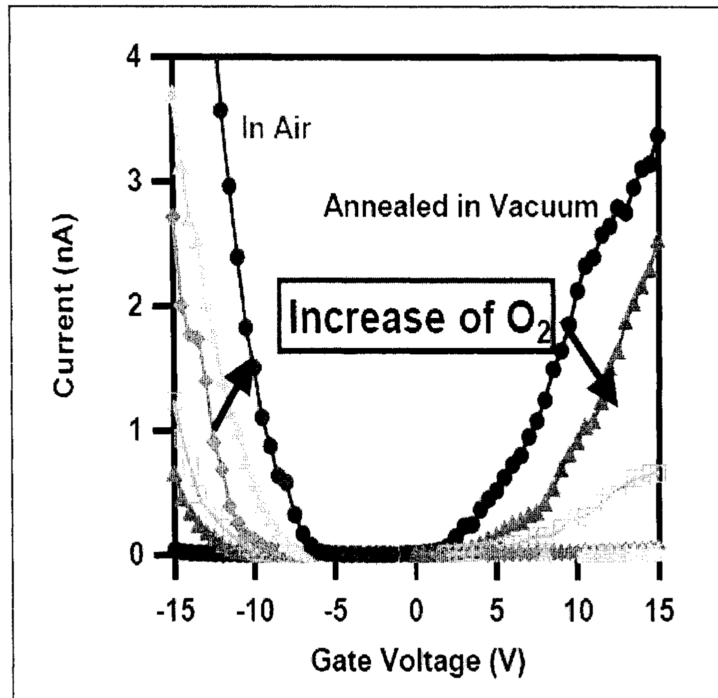

Figure 4-5: Au-contacted p-FET is converted to n-FET by annealing. [12]

For CNFETS, by simulating the situation in such a way that the current is controlled by interfaces and is dominated by the Schottky barriers we can obtain regular output characteristics for a given gate voltage. While the output characteristics of the CNFETs are comparable to those of Schottky barrier MOSFETs, the physics behind its functioning is different. In the case of Schottky Barrier MOSFETs the current is exponentially dependent on the voltage and the thermal emission over the barrier dominates in the room temperature and the scattering takes place in the channel.

For the carbon nanotube field effect transistor case, there is no scattering in the channel region and the current depends only on the interfaces. Tunneling through the Schottky barriers dominates the current because of the nanometer size of the device.

These barriers are thin enough for effective tunneling even at room temperature for almost any gate voltage.

By increasing the drain voltage for any constant gate voltage, current between source and drain increases, see Figure 4-6. At high negative gate voltage current blocks for electrons and hole current dominates in the system. For the positive gate voltage, the valence band of the carbon nanotube gets closer to the Fermi level and since electrons can tunnel through the Schottky barrier between the source and the electron current dominates in the system.

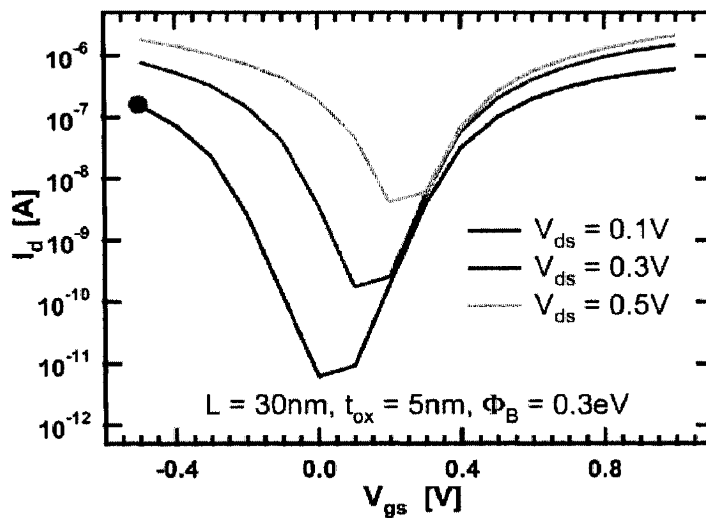

Figure 4-6: The source and drain current versus the gate voltage for three different values of the voltage between source and drain. [2]

As can be seen in Figure 4-7, at some point the barrier between the drain and channel disappears and current does not change that much by changing the drain voltage. At this point for large enough drain voltage, V_{ds}, current can reach to its saturation point,see the solid line energy band in Figure 4-7. If the metal Fermi level (in case of zero V_{ds}) does not fall in the center of the band gap of the carbon nanotube Schottky Barrier's height for electrons and holes would be different.

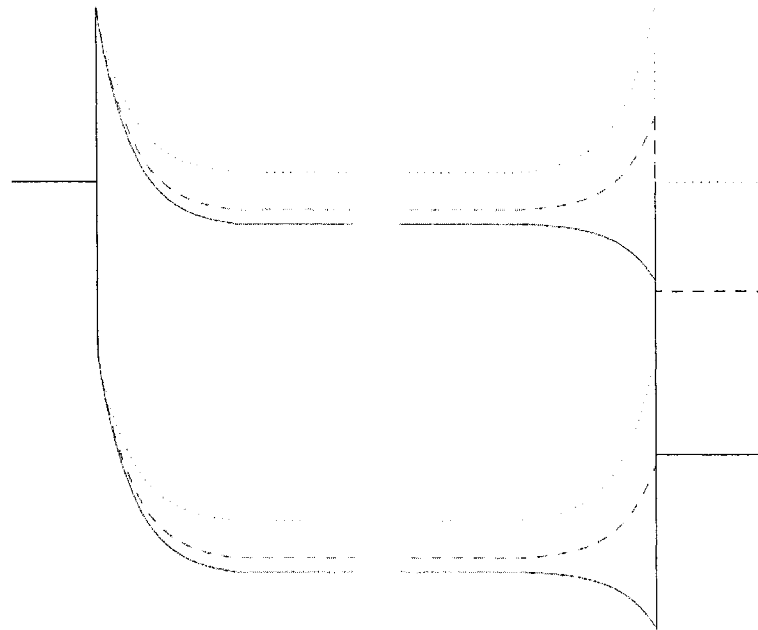

Figure 4-7: Conduction and valance energy bands diagram of the CNFET. [13]

4.3. The impact of the channel thickness on CNFET characteristics:

As mentioned before all carbon-carbon bonds are satisfied in carbon nanotubes and as a consequence, they have no interface associated with oxides. In order for the gate voltage to modulate the tunneling barrier at the source end as strongly as possible the gate-channel capacitance must be very high. Because there is no interface associated with the dielectric many types of dielectrics can be used in CNFETs.

As can be seen in the Figure 4-8, the thinner the carbon nanotube channel thickness, the thinner the tunneling barrier between the metal-carbon nanotube junction will be. As mentioned before the energy band-gap of a CNT is inversely proportional to the nanotube diameter. Therefore with larger diameter of the nanotube, which means smaller band-gap, the Schottky barrier formed at the metal-carbon nanotube junction will be smaller.

Consequently, this leads to a larger current, but at the same time the off-current would be higher.

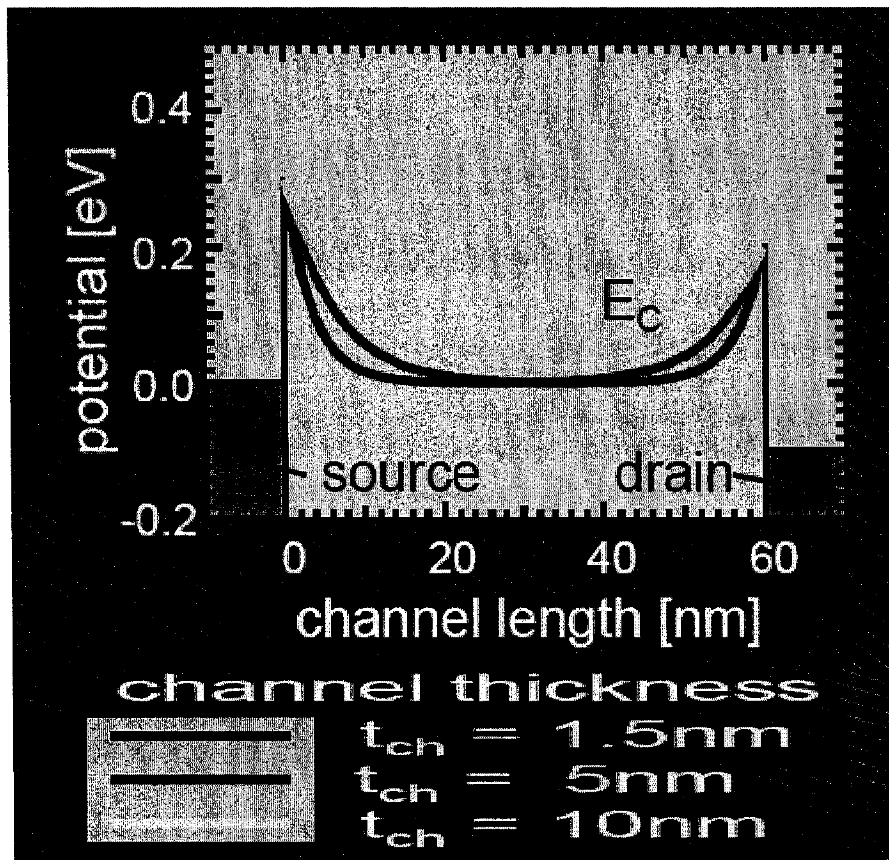

Figure 4-8: The impact of the body thickness on tunneling barrier. [2]

The threshold voltage also varies by changing the nanotube diameter. In the case of p-type carbon nanotube channel, the threshold voltage of the CNFET occurs when the valence band of the tube gets equal to the source Fermi level .For the n-type carbon nanotube channel, the threshold voltage occurs when the conduction band of the tube gets equal to the Fermi level of the metal source. Because the bandgap is smaller for the larger nanotube diameter, the conduction or valence band of the tube becomes sooner equal to the source Fermi level and therefore its threshold voltage will be smaller in the magnitude, see Figure 4-9.

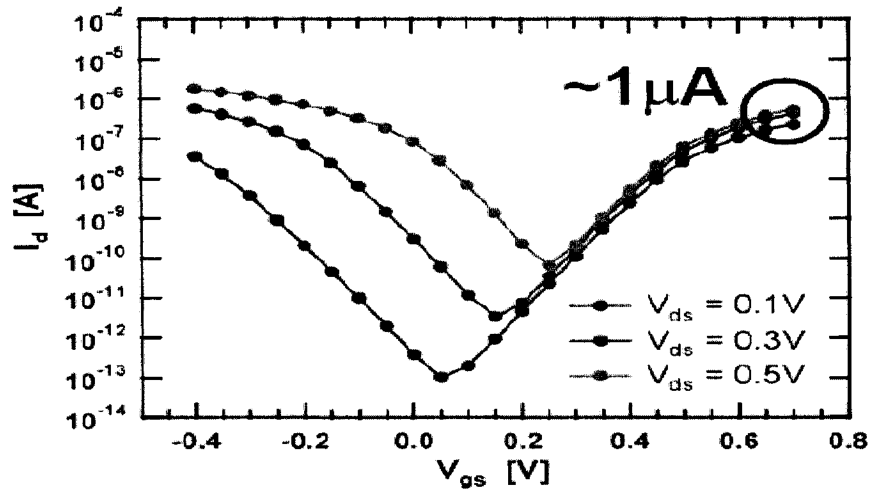

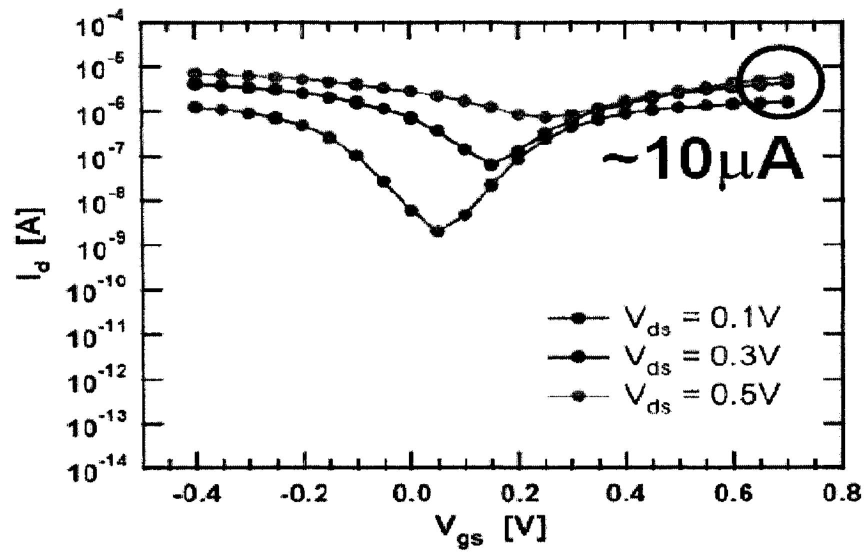

Figure 4-9: Drain current versus gate voltage for two CNT channels with different diameter, t_{ch}=1.3 nm and t_{ch}=2.5 nm respectively both for the oxide thickness, t_{ox}=2 nm. . [12]

As can be seen in Figure 4-9, the off current of the smaller diameter of the carbon nanotube is significantly lower than the off current of the diameter nanotube.

CNFETS are comparable to MOSFETs; however new fabrication technology is not at the production level.

Further scaling of these transistors is still a remaining problem. Industry is eagerly looking forward to production of experimental carbon nanotube chips as we need to go to the direction of more complex circuits.

Chapter 5
CNFET under Equilibrium Condition

Metal-Semiconductor junctions play a crucial role in electronic devices. Any desired barrier height for the Schottky barrier can be obtained by using a metal with appropriate work function. From an application point of view in nanotube studies, transistor is the most interesting subject to study theoretically. It is not yet clear how carbon nanotube field effect transistor operates. For nanoscale devices based on carbon nanotubes or other linear molecules, it seems that contacts will play a crucial role because the entire device may lie within nanometers of the interface. For simplicity, the discussion is restricted to the barrier for electrons; a trivial modification gives the barrier for holes.

Most of the metal-carbon nanotube junctions that have already been studied employ a weak Van der Waals side contacts, see Figure 5-1(a). However, in real applications an end-bonded junction with strong (metallic-covalent) bonding will be preferable for compactness and for robust electrical contact, as discussed by Zhang et al.[10] ,and such junctions have been already fabricated .

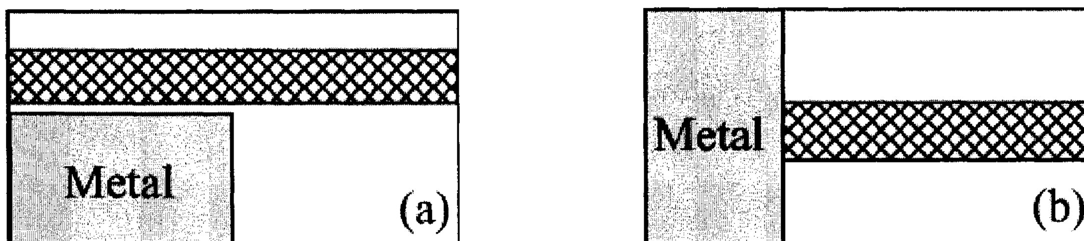

Figure 5-1: There are two types of nanotube /metal contacts: (a) nanotube side contacted by the metal by Van der Waals adhesion; (b) nanotube end bonded to the metal (covalent/metallic bonding) [14].

5.1. Carbon Nanotube Electrostatics:

Examining the electrostatics of coaxial carbon CNFETs is a first step toward obtaining its potential profile .The potential on the nanotube must be computed self consistently with the electron charge induced on the surface of the nanotube by the gate voltage. The nanotube which is considered here is intrinsic. As mentioned before, the potential in the body of the tube, distal from the contacts, depends directly on gate voltage (Vgs), leading to potential spikes at the source and drain ends.

The concentration of this work is on a coaxial geometry of the CNFET shown in Figure 5-2.The device is formed with a (16, 0) intrinsic carbon nanotube, which is a zigzag nanotube, with radius R_{cn}=0.63 nm, and length of L_{cn}=100 nm. Carbon nanotube is surrounded by insulating material and gate contact.

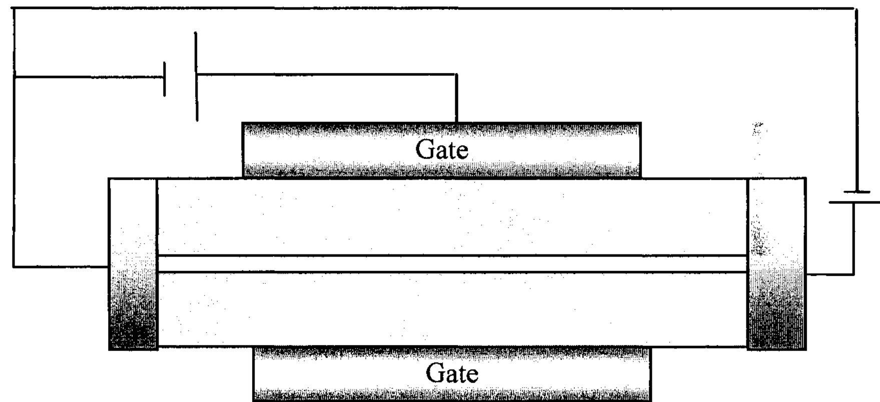

Figure 5-2: Coaxially gated carbon nanotube transistor structure.

The band gap of nanotube for this specific radius is assumed to be E_g= 0.64 eV .Also the Affinity of nanotube is χ= 4.18 eV and its work function is ϕ_{cn}=4.5 eV [4].

Relative to the Fermi level in the metal, the Fermi level in the semiconductor, which in our case is carbon nanotube, is lowered by the amount equal to the difference between the two work functions. When metal is brought into the intimate contact with the semiconductor, the Fermi levels of the two materials become coincident at thermal equilibrium. Consequently, the conduction and valence band of the semiconductor will have a definite energy relationship with the Fermi level in the metal. Once this relationship is known, it serves as a boundary condition on the solution of the Poisson equation in the semiconductor.

The tube wall is taken to be infinitesimally thin. The work functions of the tube, $\phi_{nanotube}$, and the gate, source, and drain metallization, ϕ_g,ϕ_s, ϕ_d, respectively are taken to be 4.5 eV, unless otherwise stated. Because of the use of an intrinsic nanotube, the Fermi levels of the source and drain metals lie in the middle of the nanotube's band gap. In the absence of gate leakage, equilibrium occurs when there is no voltage between source and drain($V_{dS} = 0$).

For equilibrium condition, the carrier concentrations are found by allowing the local electrostatic potential to rigidly shift the carbon density of states.

We must use the density of allowed energy states for a one dimensional carbon nanotube in order to calculate the electron and hole concentration in it. Figure 5-3 shows a one dimensional plot of allowed quantum states as a function of k. Each point represents an allowed quantum state. Positive and negative values of k have the same energy and represent the same energy states and since negative values of k do not represent additional quantum states, the density of quantum sates will be determined by considering only the positive half of the linear k space as shown in Figure 5-3.

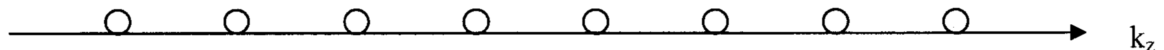

Figure 5-3: A one dimensional array of allowed quantum states in k space.

The distance between two quantum states in the k_z direction, is given by $\frac{2\pi}{a}$,therefore in k_z space there are $\frac{2dK}{\frac{2\pi}{a}} = dN$ quantum states.

The factor, 2, takes into account the two spin states allowed for each quantum state. Thus *g(E)* ,the density of states per unit length becomes:

$$DOS = g(E) = \frac{1}{a}\frac{dN}{dE} = \frac{1}{\pi}\frac{dK}{dE}$$
$$E \approx \frac{\hbar^2 k^2}{2m^*} \Rightarrow g(E) = \frac{1}{h}\sqrt{\frac{2m^*}{E}} \frac{states}{m.eV} \quad (5.1)$$

g(E) is the number of quantum sates per unit length per unit energy, m^* is the effective mass of the carrier in nanowire and *h* is Dirac's constant.

Results are presented here for the equilibrium situation, i.e., the drain-source voltage, Vds, is zero since this is the only case that carrier distribution can be calculated with certainty. Here we adopt an approach in which the effect of the gate voltage is to move the bands of the nanotube rigidly up and down.

5.2 Concentration of electrons

The distribution of electrons in the conduction band of the carbon nanotube acting as a channel in Figure 5-2 can be calculated by the integrating the density of allowed quantum states times the probability that a state is occupied by an electron over the entire conduction-band energy. Placing the Fermi level, E_f=0:

$$Q_z(z') = q\int_0^{+\infty} dE.g(E).f(E) \quad (5.2)$$

Where in equation (5.2), $g(E)=\frac{dN}{dE}=\frac{1}{h}\sqrt{\frac{2m}{E-E_c}}=\frac{1}{h}\sqrt{\frac{2m^*}{E-E_c}}$ is the density of states of the conduction band per unit of energy in one dimension, see equation (5.1).

m* is the effective electron mass in the carbon nanotube: $m^* = 0.06\times 9.11\times 10^{-31} Kg$ [21], h is the Planck's constant .

E_c , the bottom edge of the conduction band, at each point in z direction along the tube can be defined as $E_c(z') = E_{cmid} + qV(z')$, in which $qV(z')$ is the amount of band bending near the source or drain at each end of CNFET. The basic premise is that there exists a region in the mid-length of the tube in which the potential energy is relatively flat, $E_{cmid,}$ and serves to connect the regions of rapidly varying potential energy close to the end contacts because of the Schottky barriers.

A constant E_{cmid} is commensurate with a constant charge in the mid-length region of the nanotube.

$f(E) = \frac{1}{1+\exp(\frac{E-E_F}{kT})}$ in equation (5.2) is called the Fermi-Dirac distribution function and gives a probability that a quantum state is occupied by an electron.

For the equilibrium condition, the charge density at any point like z' near the source contact along the carbon nanotube channel can be written as:

$$Q_z(z') = q\int_{E_c}^{\infty} dE.g_{z'}(E).f_{z'}(E) = q\int_{E_c(z')}^{\infty}\frac{1}{h}\sqrt{\frac{2m^*}{E-E_c(z')}}.\frac{1}{1+\exp(\frac{E-E_F}{kT})}.dE$$

$$= Q_z(z') = q\int_{E_c(z')}^{\infty}\frac{1}{h}\sqrt{\frac{2m^*}{E-E_c(z')}}.\frac{1}{1+\exp(\frac{E}{kT})}.dE \qquad (5.3)$$

Where Fermi energy level, E_F, is taken to be zero.

In order to simplify equation (5.3), taking $E - Ec(z') \rightarrow E$, it becomes:

$$Q_z(z') = q\int_0^\infty \frac{1}{h}\sqrt{\frac{2m^*}{E}}.\frac{1}{1+\exp(\frac{E+E_c(z')}{KT})}.dE \quad (5.4)$$

Having $E + E_c(z') = E + E_{cmid} + qV(z') >> kT$, the Maxwell-Boltzmann approximation can be used in (5.4) .This is a reasonable assumption remembering that the band gap energy of the carbon nanotube is around 0.6 eV and by neglecting the very high gate voltage.

Therefore the value of the charge at each point like z' near the contacts can be calculated as:

$$Q_z(z') = q\int_0^\infty \frac{1}{h}\sqrt{\frac{2m^*}{E}}\frac{1}{1+\exp(\frac{E+E_c(z')}{kT})}dE = q\int_0^\infty \frac{1}{h}\sqrt{\frac{2m^*}{E}}\exp(\frac{-(E+E_c(z'))}{kT})dE =$$
$$\frac{q}{h}\sqrt{2m^*}\int_0^\infty E^{\frac{-1}{2}}.\exp(\frac{-(E+E_c(z'))}{kT}).dE = \frac{q}{h}\sqrt{2m^*}\exp(\frac{-E_c(z')}{kT})\int_0^\infty E^{-\frac{1}{2}}.\exp(\frac{-E}{kT})dE \quad (5.5)$$

The integral of equation (5.5) may be solved more easily by making a change of variable. If we let

$$\frac{-E}{kT} \rightarrow \eta \Rightarrow -dE = d\eta$$

Then the integral in equation (5.5) becomes

$$\int_0^\infty E^{-\frac{1}{2}}.\exp(\frac{-E}{kT})dE = \int_0^\infty (kT\eta)^{-\frac{1}{2}}.\exp(-\eta)(kTd\eta)$$
$$= (kT)^{\frac{-1}{2}}.(kT)\int_0^\infty \eta^{\frac{-1}{2}}\exp(-\eta)d\eta = (kT)^{\frac{1}{2}}\int_0^\infty \eta^{\frac{-1}{2}}.\exp(-\eta)d\eta \quad (5.6)$$

The integral is the gamma function, with a value of

$$\Gamma(x) = \int_0^\infty t^{x-1} e^{-t} dt \Rightarrow \Gamma(\frac{1}{2}) = \int_0^\infty \eta^{\frac{-1}{2}} e^{-\eta} d\eta = \sqrt{\pi}$$

Therefore equation (5.5) can be written as

$$Q_z(z') = \frac{q}{h}\sqrt{2m^* KT\pi}\exp(\frac{-E_c(z')}{KT}) \qquad (5.7)$$

As mentioned before the bottom edge of the conduction band, $E_c(z')$ at each point in z direction along the tube can be defined as $E_c(z') = E_{cmid} + qV(z')$, in which $qV(z')$ is the amount of band bending near the source or drain at each end of CNFET.E_{cmid} is the conduction band edge at some point in the middle of the CN where the band edge goes flat.

Then equation (5.7) becomes

$$Q_z(z') = \frac{q}{h}\sqrt{2m^* KT\pi}\exp(\frac{-E_c(z')}{KT}) =$$
$$\frac{q}{h}\sqrt{2m^* KT\pi}\exp(\frac{-Ecmid}{kT}).\exp(\frac{-qV(z')}{kT}) \qquad (5.8)$$

We may define parameter A as

$$A = \frac{q}{h}\sqrt{2m^* KT\pi}\exp(\frac{-E_{cmid}}{KT})$$

So the carrier concentration can be written as

$$Q_z(z') = A.\exp(\frac{-qV(z')}{KT}) \qquad (5.9)$$

Having

$q = 1.6\times10^{-19}C, h = 6.625\times10^{-34} j-s, kT = 0.0259eV, m^* = 0.06\times9.11\times10^{-31}Kg$ .For example in the CNFET, if we apply a 0.2 V gate voltage, V_{gs}, it can push the conduction band to E_{cmid}=0.1 eV.

Therefore, A, in equation (5.9) becomes

$$\therefore A =$$

$$\frac{q}{h}\sqrt{2m^* KT\pi}\exp(\frac{-E_{cmid}}{KT}) = \frac{-1.6\times10^{-19}}{6.625\times10^{-34}}\sqrt{2\times0.06\times9.11\times10^{-31}\times0.0259\times1.6\times10^{-19}\times\pi}\exp(-\frac{0.1}{0.0259})$$

$$=1.19\times10^{6}\frac{e}{m} = -1.6\times10^{-19}\times1.19\times10^{6}\frac{C}{m}$$

=>

$$Q_z(z') = -1.917\times10^{-13}.\exp(\frac{-qV(z')}{KT})\left[unit = \frac{C}{m}\right]$$

$$= -1.917\times10^{-22}.\exp(\frac{-qV(z')}{KT})\left[unit = \frac{C}{nm}\right] \qquad (5.10)$$

Equation (5.10) gives the net 1-D carrier density at some point along the intrinsic tube in the CNFET. As can be seen in equation (5.10), the amount of charge near the source and drain is exponentially dependent on the amount of the Schottky barrier band bending, *qV(z')*, which decreases as its distance from the source and drain increases.

From equation (5.8), by considering zero band banding ($qV(z') = 0$), we can calculate the electron charge density at the mid conduction band for different gate voltages, see Figure 5-4. By increasing the gate voltage, the Fermi level of the nanotube gets closer to its conduction band and the electron density vs. gate voltage increases exponentially.

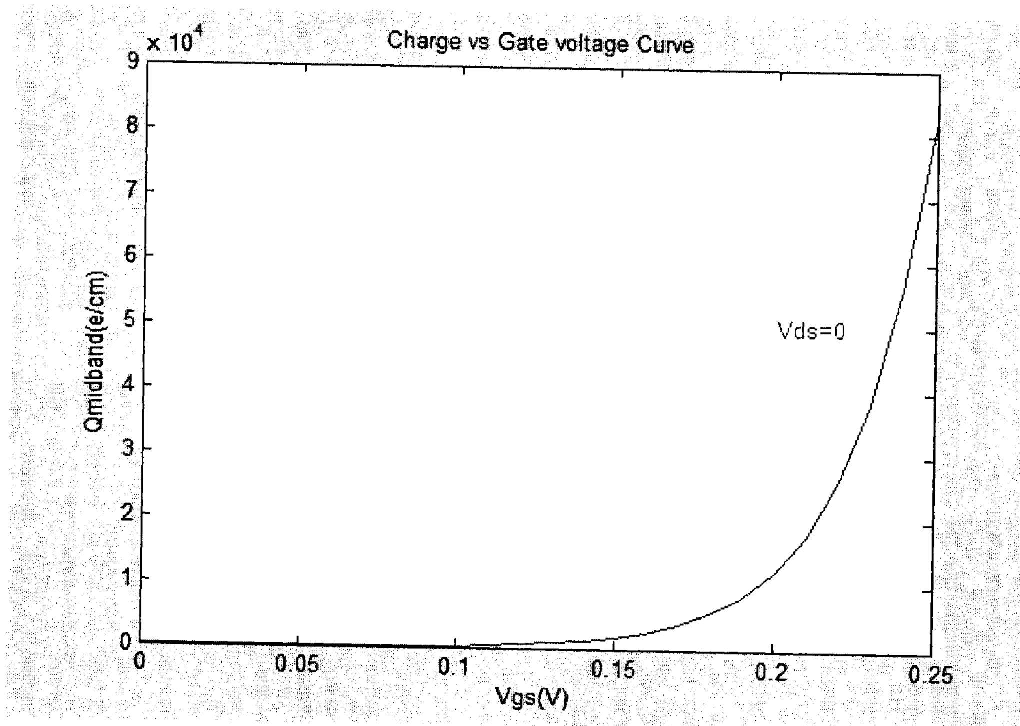

Figure 5-4: Electron density at the mid band of the carbon nanotube versus gate voltage where Maxwell-Boltzmann approximation is applicable.

5.3 Concentration of holes

The concentration of holes in the valence band is found by integrating the density of allowed quantum states in the valence band multiplied by the probability that a state is not occupied by an electron:

$$Q_z(z') = \int_{-\infty}^{E_v(z')} g_v(E).[1-f_F(E)]dE = \int_{-\infty}^{E_v(z')} \frac{1}{h}\sqrt{\frac{2m^*}{E_v(z')-E}}\frac{1}{1+\exp(E_F-E)}dE \qquad (5.11)$$

Where $g_v(E) = \frac{dN}{dE} = \frac{1}{h}\sqrt{\frac{2m^*}{E_v - E}}$ is the density of states of the valence band in one dimension and m* is the effective mass of the holes in carbon nanotube and $f(E) = \frac{1}{1+\exp(\frac{E-E_f}{kT})}$ is the Fermi-Dirac distribution function.

We have to consider the effect of the Schottky barrier at source and drain end of the carbon nanotube on the valence energy band. Valence energy band at each point along the carbon nanotube becomes $E_v(z) = E_{vmid} + qV(z)$, where $qV(z)$ is the amount of the band bending of the valence band near the source or drain end of the CNFET. E_{vmid} is the valence band edge at some point in the middle of the CN where it goes flat.

The integral of equation (5.11) may be solved more easily by making a change of variable. If we let

$E_v(z') - E \rightarrow E$

Then equation (5.11) becomes:

$$Q_z(z') = \int_{-\infty}^{0} g_v(E).[1-f_F(E)]dE = \int_{-\infty}^{0} -\frac{1}{h}\sqrt{\frac{2m^*}{E}}\frac{1}{1+\exp(E_F - E_v(z') + E)}dE \qquad (5.12)$$

The Fermi probability function reduces to the Boltzmann approximation so equation (5.12) becomes

$$Q_z(z') = \int_0^\infty \frac{1}{h}\sqrt{\frac{2m^*}{E}} \exp(\frac{E_v(z') - E}{kT}) dE \tag{5.13}$$

Using the gamma function definition ,equation (5.13) becomes

$$Q_z(z') = \sqrt{\frac{2m^* kT\pi}{h^2}} \exp(\frac{E_v(z')}{kT}) \tag{5.14}$$

As mentioned before valence band at each point along the nanotube can be written as $E_v(z') = E_{vmid} + qV(z')$, where $qV(z')$ is the amount of band bending of the valence band near the source or drain end of the CNFET. E_{vmid} is the valence band edge at some point in the middle of the CN valence band where the band edge goes flat.

Therefore equation (5.14) becomes

$$Q_z(z') = \sqrt{\frac{2m^* kT\pi}{h^2}} \exp(\frac{E_{vmid}}{kT}) \exp(\frac{qV(z')}{kT}) \tag{5.15}$$

We may define parameter B as

$$B = \frac{1}{h}\sqrt{2m^* KT\pi} \exp(\frac{E_{cvmid}}{KT})$$

So equation (5.15) can be written as

$$Q_z(z') = B.\exp(\frac{qV(z')}{KT}) \tag{5.16}$$

Because of the symmetric structure of SWCNT valence and conduction bands, electrons and holes have essentially the same band structure and consequently nearly the same effective mass.

Having $q = 1.6\times10^{-19}, h = 6.625\times10^{-34}\, j-s, kT = 0.0259eV, m^* = 0.06\times9.11\times10^{-31}$

V_{gs} is considered to be 0.2 V which result in E_{vmid}=-0.5 eV.

So, B, in equation (5.16) becomes

$$\therefore B = \frac{q}{h}\sqrt{2m^*KT\pi}\exp(\frac{E_{vmid}}{KT}) =$$

$$\frac{1.6\times10^{-19}}{6.625\times10^{-34}}\sqrt{2\times0.06\times9.11\times10^{-31}\times0.0259\times1.6\times10^{-19}\times\pi}\exp(-\frac{0.5}{0.0259}) = 0.23\frac{\#h}{m}$$

=>

$$Q_z(z') = 3.76\times10^{-20}.\exp(\frac{qV(z')}{KT})\left[unit = \frac{C}{m}\right] = 3.76\times10^{-29}.\exp(\frac{qV(z')}{KT})\left[unit = \frac{C}{nm}\right] \quad (5.17)$$

As can be seen in equation (5.17), carrier charge density near the source and drain is exponentially dependent on the amount of the Schottky barrier band bending, *qV(z')*, which increases as its distance from the source and drain decreases.

From equation (5.15), by considering zero band banding ($qV(z') = 0$), we can calculate hole charge density at the mid valence band for different gate voltages. By increasing the gate voltage, the Fermi level of the nanotube gets closer to its conduction band and the hole density decreases exponentially, see Figure 5-5.

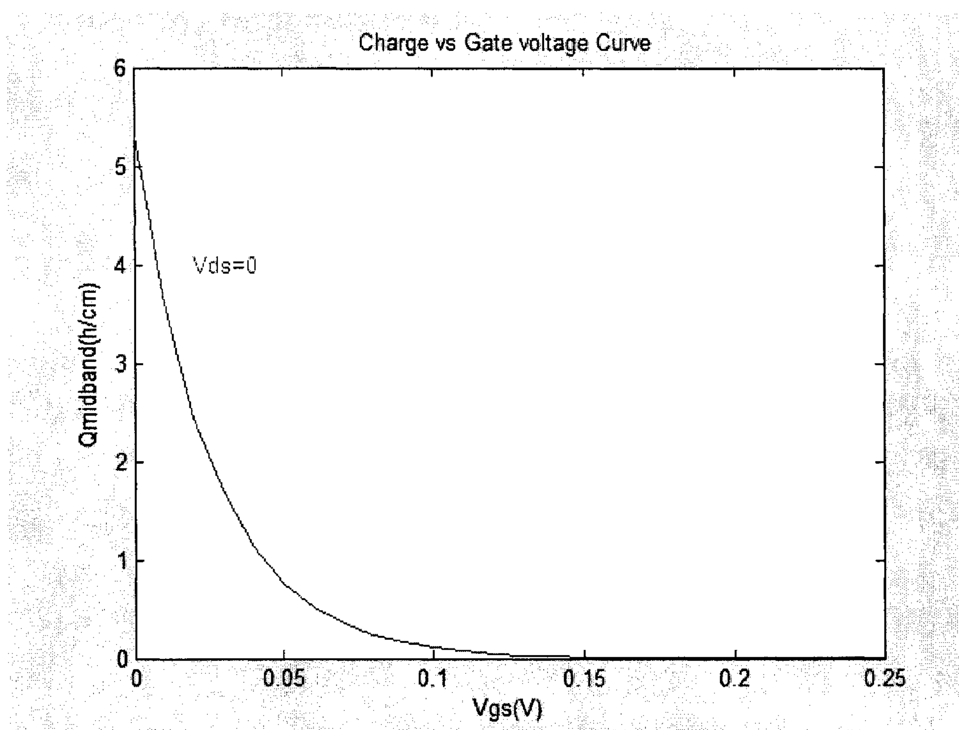

Figure 5-5: Carrier density at the mid valence band of the carbon nanotube versus Gate voltage where Maxwell-Boltzmann approximation is applicable.

Charge density versus gate voltage graph at the mid band of the carbon nanotube for both electrons and holes confirms that by increasing the gate voltage, the Fermi level of the nanotube gets closer to its conduction band and the electron density vs. gate voltage increases exponentially when at the same time the hole density exponentially decreases.

In case of low gate voltage, for example Vgs = 0.2 V, which result in E_{cmid}=0.1 eV and E_{vmid}=-0.5eV total concentration can be written as:

$$Q(z') = [1.19\times10^{6}\times\exp(\frac{-qV(z')}{KT})\frac{\#e}{m} - 0.23\times\exp(\frac{qV(z')}{KT})\frac{\#h}{m}]\left[unit = \frac{C}{m}\right] \tag{5.18}$$

As can be seen in equation (5.18), charge density near the source and drain is exponentially dependent on the amount of the Schottky barrier band bending at each point like z' along the nanotube($qV(z')$). Energy band diagram versus charge density at source and drain end of the carbon nanotube graph confirms that the electron density increases as the Schottky barrier bending decreases, see Figure 5-6.

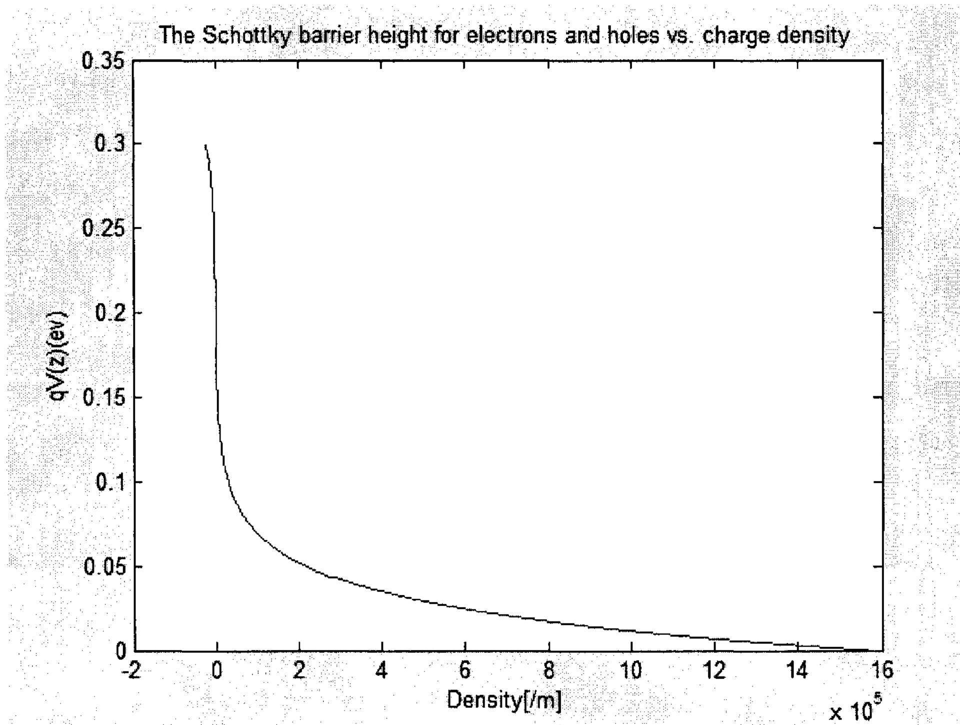

Figure 5-6: Energy band diagram versus charge density of a metal-carbon nanotube junction.

In the derivation of the equation (5.2) and (5.11) for the equilibrium electron and hole concentrations, we assumed that the Boltzmann approximation was valid. If the Boltzmann approximation does not hold, the concentration of electrons without using Boltzmann approximation can be written as:

$$Q_z(z') =$$

$$q\int_0^{\infty}\frac{1}{h}\sqrt{\frac{2m^*}{E}}\frac{1}{1+\exp(\frac{E+E_c(z')}{KT})}dE = q\int_0^{\infty}\frac{1}{h}\sqrt{\frac{2m^*}{E}}.\frac{1}{1+\exp(\frac{E+E_{cmid}+qV(z')}{KT})}dE$$

$$\Rightarrow Q_{z'}(z) = \frac{q}{h}\sqrt{2m^*}\int_0^{\infty}E^{-\frac{1}{2}}.\frac{1}{1+\exp(\frac{E+E_{cmid}+qV(z')}{KT})}.dE$$

$$= \frac{1.6\times10^{-19}}{6.625\times10^{-34}}\sqrt{2\times0.06\times9.11\times10^{-31}}\times\sqrt{1.6\times10^{-19}}\int_0^{\infty}E^{-\frac{1}{2}}.\frac{1}{1+\exp(\frac{E+E_{cmid}+qV(z')}{KT})}.dE$$

$$= 3.194\times10^{-11}\int_0^{\infty}E^{-\frac{1}{2}}.\frac{1}{1+\exp(\frac{E+E_{cmid}+qV(z')}{KT})}.dE \qquad (5.19)$$

From equation (5.19), by considering zero band banding ($qV(z') = 0$), we can calculate the electron charge density at the mid conduction band for different gate voltages. By increasing the gate voltage, the Fermi level of the nanotube gets closer to its conduction band and the electron density vs. gate voltage increases exponentially, see Figure 5-7.

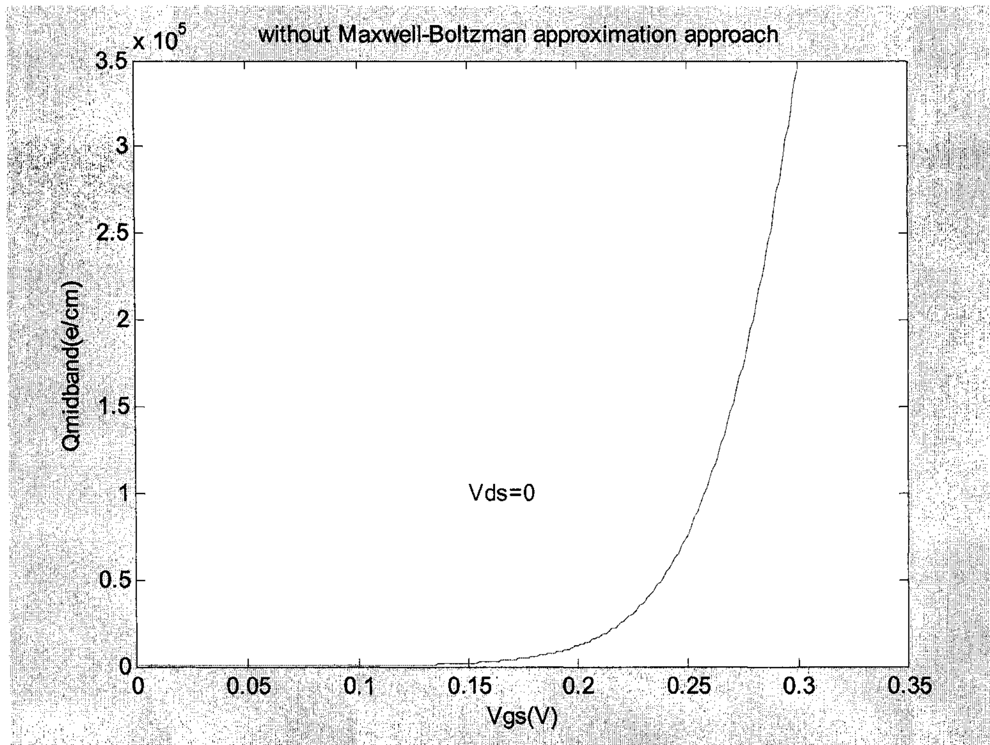

Figure 5-7: Electron density at the mid band of the carbon nanotube versus gate voltage where Maxwell-Boltzmann approximation is not applicable.

Comparing two graphs with different approaches to the charge equation shows the similar result .This suggests that the Maxwell-Boltzmann approximation can be used as a good estimation for determining the carbon nanotube charge for the mid band of the nanotube at low voltages.

5.4. The energy diagram of the conduction band without using the Maxwell-Boltzmann approximation:

The electric field in the space charge region of the metal-carbon nanotube junction is determined from the Poisson's equation (for abrupt approximation):

$$\frac{\partial^2 V(z)}{\partial z^2} = -\frac{Q(z)}{\varepsilon_s} \tag{5.20}$$

Where $V(z)$ is the electric potential. $Q(z)$ is the space charge density and ε_s is the permittivity of the carbon nanotube. The dielectric constant for quasi-one-dimensional and two-dimensional semiconductors is equal to one [42].

Equation (5.20) gives the electric potential at any point like z along the nanotube. Charge at each particular point like z is distributed around $2\pi R_{cn}$ therefore $Q(z)$ has to be divided by $2\pi R_{cn}$ and consequently should be solved self consistently with the Poisson equation (5.20) .Therefore the potential profile can be computed and graphed, see Figure 5-8.

In order to confine the charge to the carbon nanotube surface, we need to multiply the charge value by the delta function $\delta(R - R_{cn})$ which is equal to one only when $R=R_{cn}$.

As an example for this method we can consider the energy band diagram for the carbon in CNFET in which the conduction band be at E_{cmid}=0 eV and the valence band be E_{vmid} =-0.6 eV .As mentioned before we considered a carbon nanotube with the radius R_{cn}=0.63 nm

Therefore placing E_F=0, charge density becomes

$$Q(z')=$$

$$\frac{1}{2\pi R_{cn}}\delta(R-R_{cn})[-3.194\times10^{-11}\int_0^{\infty}E^{-\frac{1}{2}}.\frac{1}{1+\exp(\frac{E+E_{cmid}+qV(z')}{kT})}.dE+3.76\times10^{-20}.\exp(\frac{qV(z')}{kT})]$$

$$;R=R_{cn}$$

$$\Rightarrow Q(z')=$$

$$\frac{1}{2\pi(0.63)}[-3.194\times10^{-20}\int_0^{\infty}E^{-\frac{1}{2}}.\frac{1}{1+\exp(\frac{E+qV(z')}{kT})}.dE+7.92\times10^{-22}.\exp(\frac{qV(z')}{kT})]\left[unit=\frac{C}{nm}\right] \quad (5.21)$$

In this example we assumed E_{cmid}=0 eV. This means that the Fermi level energy band coincides with the conduction band. Therefore the Boltzmann approximation does not hold in equation (5.21).

Using equation (5.21), nonlinear ordinary equation (5.20) is solved and *V (z)* versus distance z is obtained with the Matlab program bvp4c where V (z) varies from zero to Schottky barrier's height. At equilibrium, and by considering the same work function for source and drain, the potential profile along the tube will be symmetrical. Therefore only profile near the source end is shown here. See Figure 5-8 and 5-9.

The solution for the potential in equation (5.11) is relatively straightforward under equilibrium condition because as we saw the Fermi-Dirac statistics apply not just in the metal contacts, but everywhere along the tube and it can be used to compute the carrier concentrations.

The potential in the body of the tube, distal from the contacts, depends directly on gate voltage (V_{gs}) leading to the potential spikes in the tube at the source and drain of height determined by both work functions of source and drain and V_{gs} .Only in low metal work function, Φ_s, case and low gate voltage (V_{gs}) the thermionic emission likely to make a significant contribution to the source current; otherwise, tunneling through the spikes

dominates. The decay length for the end potential is in the order of tube's distance from gate[43].

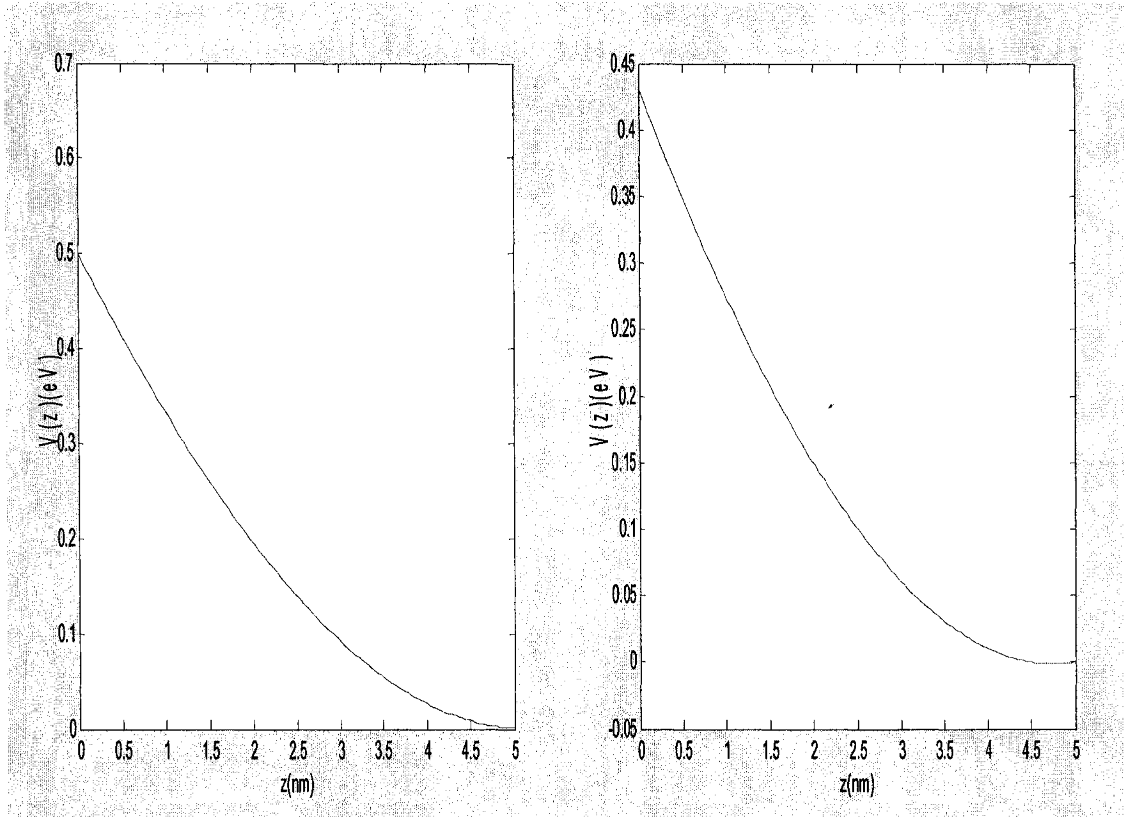

Figure 5-8: Energy band diagram near the source end without using the Maxwell-Boltzmann approximation considering the work function of carbon nanotube being equal to 4.2 eV, V_{gs}=0.3 and Φ_S=Φ_D set to

a) 4.7 eV, Φ_{bn} (Schottky barrier's height) = 4.7-4.2=0.5 eV

b) 4.63 eV, Φ_{bn} (Schottky barrier's height) = 4.63-4.2=0.43 eV

The decay length for the end potential is about 5 nm.

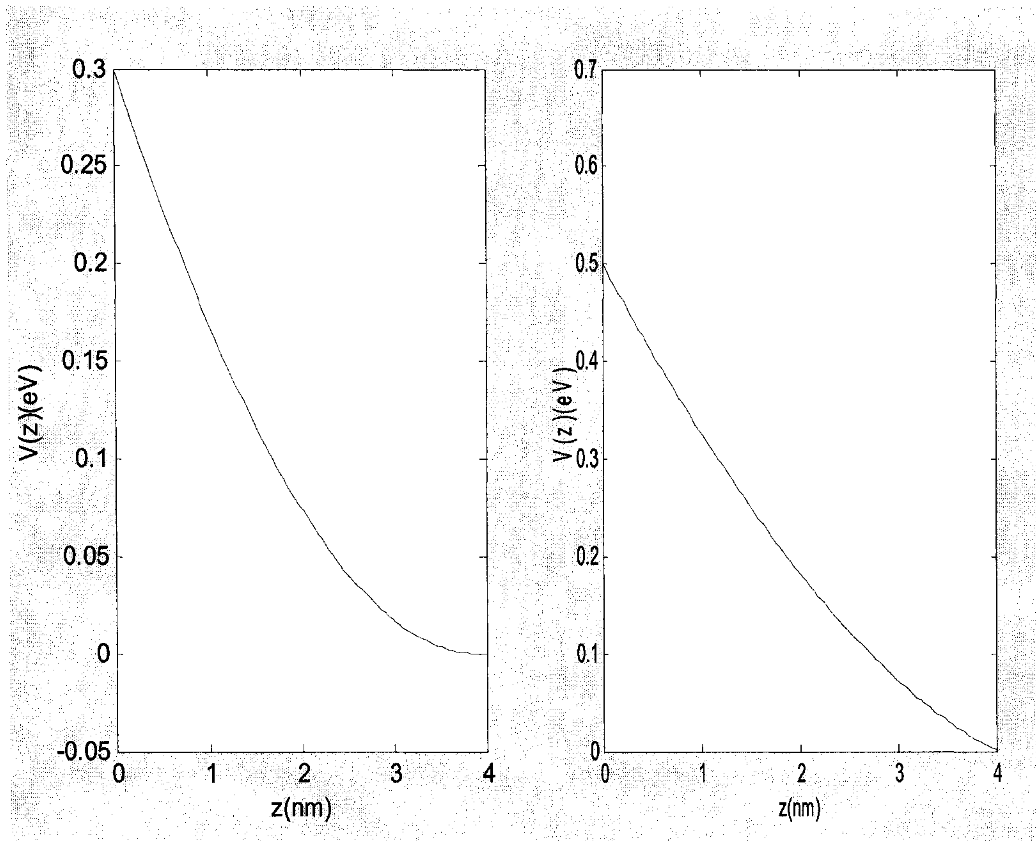

Figure 5-9: Energy band diagram near the source end without using the Maxwell-Boltzmann approximation considering the work function of carbon nanotube being equal to 4.2 eV, V_{gs}=0.3 and $\Phi_S=\Phi_D$ set to

a) 4.5 eV, Φ_{bn} (Schottky barrier's height) = 4.5-4.2=0.3 eV

b) 4.7 eV, Φ_{bn} (Schottky barrier's height) = 4.7-4.2=0.5 eV

The decay length for the end potential is about 4 nm.

5.5. Energy band diagram using Maxwell-Boltzmann approximation:

As another approach to the Poisson equation we can solve equation (5.20) considering a low gate voltage value. We assumed that because of low gate voltage, Boltzmann approximation can be valid in the charge density equation (5.21).

Assuming E_{cmid}=0.1 eV, using Maxwell-Boltzmann approximation, considering both conduction and valence band carrier densities, charge density becomes

$$Q_z(z') = -1.917\times10^{-22}.\exp(\frac{-qV(z')}{KT})\left[unit=\frac{C}{nm}\right]+3.76\times10^{-29}.\exp(\frac{qV(z')}{KT})\left[unit=\frac{C}{nm}\right] \quad (5.22)$$

Therefore Poisson equation can be written as

$$\frac{\partial^2 V(z)}{\partial z^2}=\frac{Q(z)}{\varepsilon}=0.021\exp(\frac{-qV(z')}{KT})-4.248\times10^{-9}\exp(\frac{qV(z')}{KT}) \quad (5.23)$$

The nonlinear ordinary equation (5.23) can be solved and V (z) versus distance z diagram can be obtained with the Matlab programbvp4c, see appendix2, in which V (z) varies from zero to Schottky barrier's height.

Figure 5-10 shows the Schottky barrier potential that was derived for the source-carbon nanotube junction using equation (5.23).

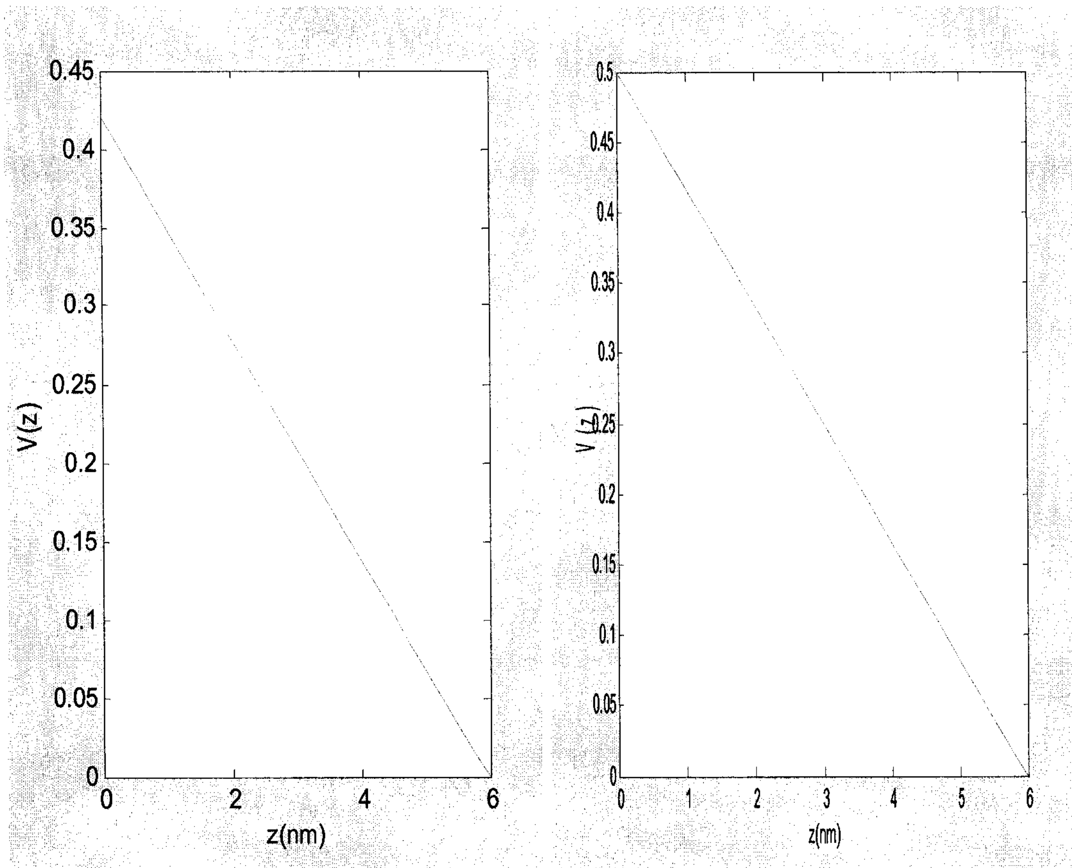

Figure 5-10: Energy band diagram near the source end using the Maxwell-Boltzmann approximation considering the work function of carbon nanotube being equal to 4.2 eV, V_{gs}=0.3 and $\Phi_S=\Phi_D$ set to

a) 4.5 eV, Φ_{bn} (Schottky barrier's height) = 4.7-4.2=0.5 eV

b) 4.63 eV, Φ_{bn} (Schottky barrier's height) = 4.63-4.2=0.43 eV

The graphs of conduction energy band near the source end of the carbon nanotube channel of CNFET, (see Figure 5-8 to 5-10), with different approaches to the charge equation are different. This can suggest that Maxwell-Boltzmann approximation is not a good estimation for determining the energy band diagrams even for low voltages.

Chapter 6

CNFET under Non-equilibrium Condition

Turning now to the non-equilibrium case for CNFET, the small number of propagating modes in the carbon nanotube is in contrast to the very large number of propagating modes in bulk terminal to which it is connected. This mode-constriction leads to a quantized, interfacial conductance, which exists even if conduction down the nanotube itself is ballistic. In the modeling of carbon nanotube diodes and field-effect transistors, it is becoming customary to locate such interfaces at the end contacts of a semiconducting nanotube, and to regard the nanotube as an object with a characteristic transmission probability T.

The end contacts are viewed as reservoirs of charge, maintained under equilibrium conditions, from which carriers are injected into the nanotube, depending on T and the applied bias, e.g. the drain-source voltage of a CNFET.

Transport over the length of the nanotube which is used in CNFETs is ballistic and the current through the transistor is calculated from the Landauer –Buttiker formula which can be defined as [32]:

$$I = \frac{4q}{h} \int T(E).\left[f(E) - f(E - qV_{ds})\right] dE \qquad (6.1)$$

Where q is the magnitude of the electronic charge, h is Planck's constant, f(E) is the Fermi-Dirac distribution function, and T refers to transmission probability of electrons. Once T (E) is known, the problem of the DC drain current is solved.

We could view the Landauer formula, equation (6.1), as a mesoscopic version of the Einstein relation:

$$\delta = e^2 N_s D \Rightarrow G = \frac{2e^2 MT}{h}$$

With the conductivity replaced by the conductance, the density of states is replaced by the number of transverse modes (or sub bands) and the diffusion constant replaced by the transmission probability:

$\delta \rightarrow G$ $\quad N_s \rightarrow M$ $\quad D \rightarrow T$

The conductance of large samples obeys an ohmic scaling law: $G = \frac{\delta W}{L}$.But as we go to the smaller dimensions there are two corrections to this law. First, there is an interface resistance independent on the length L of the sample. Second, the conductance does not decrease linearly with the width W. Instead it depends on the number of transverse modes in the conductor:

$$G = \frac{2e^2 MT}{h}$$

The factor T represents the average probability that an electron injected at one end of the conductor will transmit to the other end. M represents the number of transverse modes (or sub bands) and h is the plank's constant.

6.1. Transmission Coefficient at Source/Drain of a CNFET

Rather sophisticated method for dealing with continuous potential is the WKB approximation. For a barrier of more complicated shape like our Schottky barrier here, the Schrödinger equation can not be exactly solved, and the WKB approximation is often suited for the problem. This approach commonly known as the WKB method is also called the classical approximation.

Using this approach the transmission coefficient can be derived as [22]:

$$|Trans.coeff| \approx T = \exp\left\{\frac{-1}{\hbar}\int_{x_1}^{x_2}\sqrt{2m\left[V(x)-E\right]}.dx\right\} \tag{6.2}$$

Where *V(x)* is the potential experienced by the particle, and *E* is the total energy of the particle.

Consideration of tunneling is important for studying positive-barrier devices, as in the original presentation of the model. Two potential barriers at source and drain contact of a CNFET as a function of position is shown in Figure 6-1 and Figure 6-2.

In order to find the current value between source and drain the total transmission coefficient of a CNFET should be calculated.

The total transmission Probability for both source and drain barriers can be calculated by [22]:

$$\mathrm{T}=|t_{sd}|^2 = \frac{T_1T_2}{1+R1R2-2\cos\theta\sqrt{R_1R_2}} \tag{6.3}$$

Where T_1 is the transmission coefficient at source contact and T_2 is the transmission coefficient at drain contact of a CNFET.

Using the same approximation, the reflection coefficient R for both barriers is equal to 1-T.

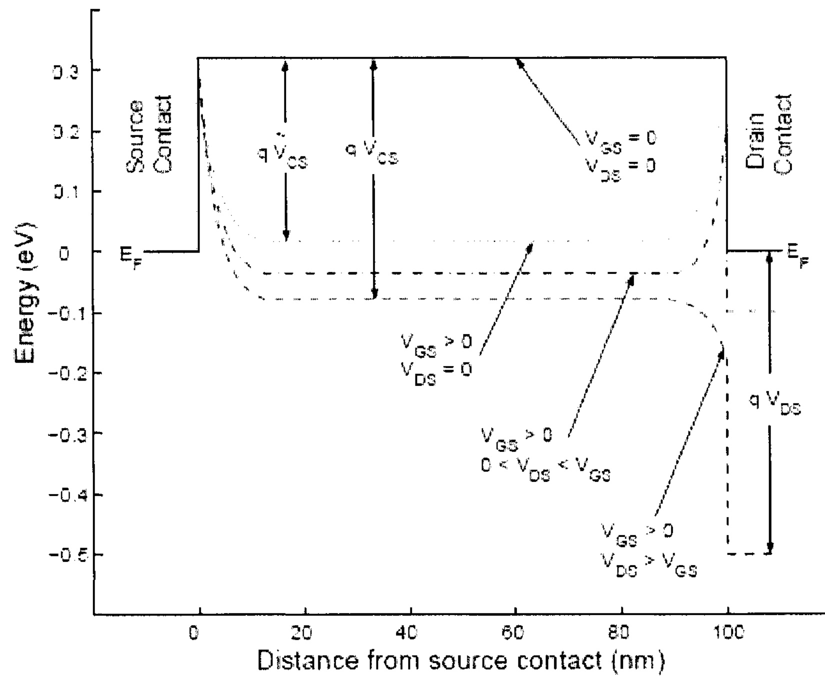

Figure 6-1: Conduction energy band diagram for various bias conditions of a CNFET [15].

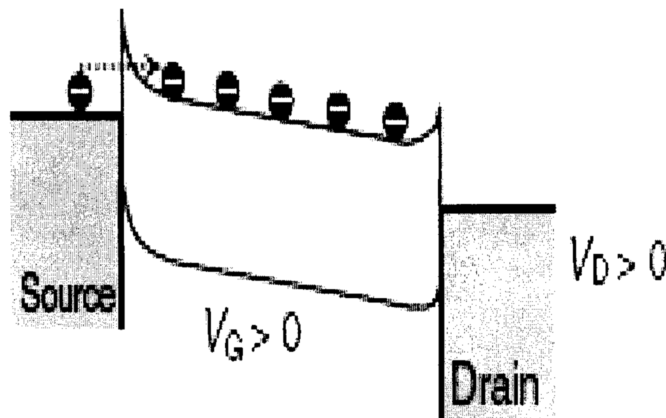

Figure 6-2: Band diagrams along the nanowire channel from source to drain for positive gate bias and positive drain bias $VD > 0$. [20]

6.1.1. Transmission Coefficient at Source-Carbon Nanotube junction of a CNFET

At non-equilibrium condition, electrons which are coming from the source reservoir to the nanotube almost experience a triangle shape barrier which is the Schottky barrier between the nanotube and the metal source that is shown by *V(x)* in the equation (6.2). This gives a solution to the tunneling probability at the source, which then can be used in computation of the drain current from Landaure's expression, equation (6.1). It is an approximate model due to the estimated shape of the barrier profiles, so the result current magnitudes given in Figure 6-5 are also only approximate.

The potential V(x) as a function of position for this problem is shown in Figure 6-3.A flux of electrons is incident on the potential source barrier and they are traveling in the +x direction.

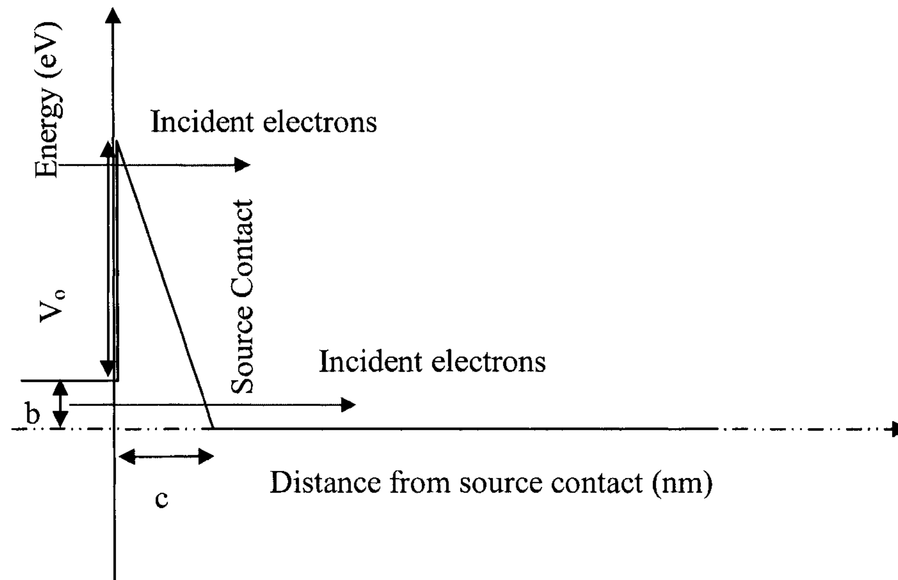

Figure 6-3: Ideal energy band diagram of the source-carbon nanotube junction of a CNFET.

The potential height is shown by V_0 in Equation (6.3).The potential function at the cource contact shown in Figure 6-3 can be approximated as:

$$V(x) = -\frac{V_0 + b}{c} x + (V_0 + b) \tag{6.4}$$

Where c is the base width of the potential barrier and b is the distance between the Fermi level of the metal and mid band of the carbon nanotube channel, see Figure 6-3.
Therefore using equation (6.2), T_1 becomes

$$T_1 = \exp\{-\frac{\sqrt{2m^*}}{\hbar} \int_{x=0}^{x=x_E} (-\frac{V_0 + b}{c} x + (V_0 + b) - E)^{\frac{1}{2}} dx\} \tag{6.5}$$

The limit of integral in Equation (6.5) is from zero to x_E. .Where x_E is the length that electrons experience potential barrier.

Form Figure 6-3, x_E, can be computed as:

$$\tan\alpha = \frac{V_0 + b}{c} = \frac{V_0 + b - E}{x_E} \Rightarrow x_E = \frac{c(V_0 + b - E)}{V_0 + b}$$

Therefore equation (6.5) can be solved as

$$T_1 = \exp\{\frac{-\sqrt{2m^*}}{\hbar}\{\frac{(\frac{(-V_0 + b)}{c} x + (V_0 + b) - E)^{\frac{3}{2}}}{\frac{3}{2}} \times \frac{-c}{V_0 + b}\}_0^{x_E}\} =$$

$$\exp\{-\frac{\sqrt{2m^*}}{\hbar}(\frac{2c}{3(V_0 + b)})\{(-\frac{(V_0 + b)}{c} x_E + (V_0 + b) - E)^{\frac{3}{2}} - (V_0 + b - E)^{\frac{3}{2}}\}\}$$

$$T_1 = \exp[\frac{-\sqrt{2m^*}}{\hbar} \times (\frac{2c}{3(V_0 + b)}) \times \{(V_0 + b - E)^{1.5}\}] \quad (6.6)$$

6.1.2. Transmission Coefficient at Drain-Carbon Nanotube junction of a CNFET

We have a flux of incident electrons originating from the source reservoir traveling in the +x direction towards the drain contact. Now we have to consider the potential barrier function at the drain contact, which is shown in Figure 6-4.The potential height of the Schottky barrier of the drain-carbon nanotube junction depends on V_{ds} (voltage between the source and drain). When a voltage bias V_{ds} is applied between the source and drain of the CNFET, the Fermi level in one of the leads becomes $E_F - qV_{ds,}$ and subsequently the potential barrier height at the drain decreases, see Figure 6-4.

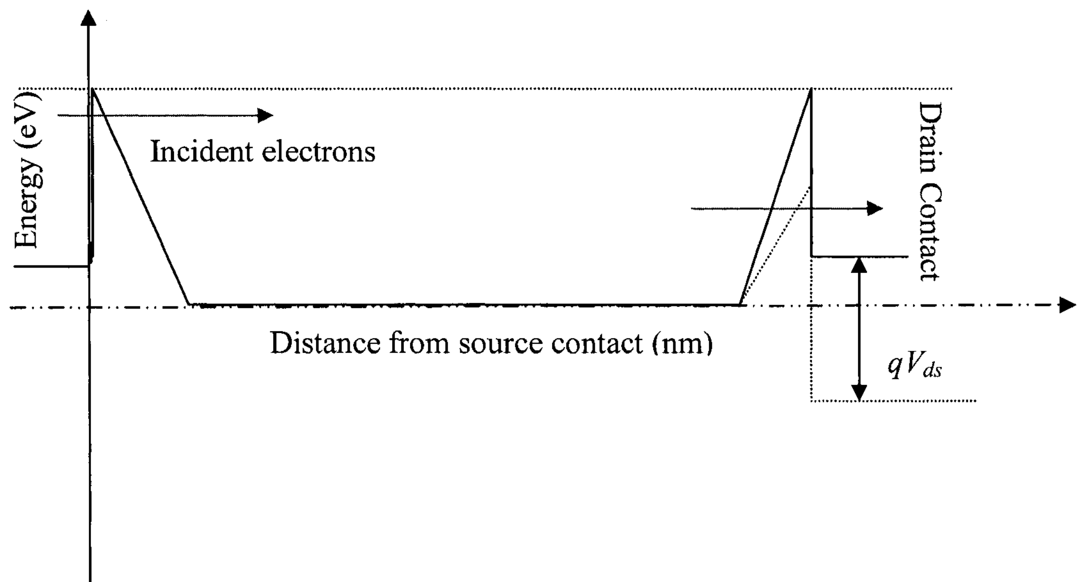

Figure 6-4: The energy band diagram of the CNFET at non-equilibrium condition. The Fermi level of the drain end lowers by the amount of the qV_{ds} (the voltage applied at source-drain ends).

T_2 can be approximated like T_1.The only difference here is that the barrier of the drain at the end of the tube is not only dependant on the work function of the contact, but it is also depends on the V_{ds}, the voltage imposed between the source and drain. The potential barrier at the drain of the nanotube diminishes as the potential between source and drain, V_{ds}, increases, see Figure 6-2 and Figure 6-4. This will lead to the saturation of the electron current. The original potential height at the drain contact when $V_{ds}=0$ is shown by V_0 in equation (6.7).The potential function at the drain contact shown in Figure 6-4 can be approximated as:

$$V(x) = \frac{V_0 + b - Vds}{c} x \tag{6.7}$$

Where c is the base width of the potential barrier at the drain contact and b is the distance between the Fermi level of the drain metal and mid band of the carbon nanotube channel.

Therefore using equation (6.2) and (6.7), T_2 becomes

$$T_2(E) = \exp\{\frac{-\sqrt{2m^*}}{\hbar} \int_{x_E}^{c} (\frac{V_0 + b - Vds}{c} x - E)^{\frac{1}{2}} dx\} \tag{6.8}$$

Where again x_E in equation (6.8) is the length that electrons experience the potential barrier. Depending on the total energy of the electron (E), x_E can have different values. From Figure 6-4, x_E can be calculated as

$$\tan\alpha = \frac{V_0 + b - Vds}{c} = \frac{V_0 + b - Vds - E}{x_E}$$

=>

$$x_E = \frac{c(V_0 + b - Vds - E)}{V_0 + b - Vds} \tag{6.9}$$

Equation (6.9) can be used as the limit of the integral (6.8) .Therefore the transmission coefficient of the drain-carbon nanotube junction, using equation (6.9), can be calculated as

$$T_2(E) = \exp\{\frac{-\sqrt{2m^*}}{\hbar} \times \frac{(\frac{V0 + b - Vds}{c}x - E)^{\frac{3}{2}}}{\frac{3}{2}} \times \frac{c}{V_0 + b - Vds}\}_{x_E}^{c}$$

$$= \exp\{\frac{-\sqrt{2m^*} \times 2c}{3\hbar(V_0 + b - Vds)}\left[(V_0 + b - Vds - E)^{1.5} - (V_0 + b - Vds - 2E)^{1.5}\right]\} \tag{6.10}$$

The total transmission Probability for both source and drain barriers can be calculated from the equation (6.3).

$$T = |t_{sd}|^2 = \frac{T_1 T_2}{1 + R1R2 - 2\cos\theta\sqrt{R_1 R_2}}$$

Here in this work we have neglected the reflections of electrons, which means that R_1 and R_2 are equal to zero in equation (6.3) and hence T would be equal to T_1T_2. WKB approximation neglects the reflection that would occur even in the absence of a barrier, so the conductance of the actual device may be somewhat lower than the WKB estimate.

Therefore the total transmission probability of CNFET using equation (6.3),(6.6) and (6.10)can be written as

$$T(E)=T1(E).T2(E)=\exp[\frac{-\sqrt{2m^*}}{\hbar}\times(\frac{2c}{3(V_0+b)})\times\{(V_0+b-E)^{1.5}\}].$$

$$\exp\{\frac{-\sqrt{2m^*}\times 2c}{3\hbar(V_0+b-Vds)}\left[(V_0+b-Vds-E)^{1.5}-(V_0+b-Vds-2E)^{1.5}\right]\} \quad (6.11)$$

6.2. I-V Characteristics of CNFET

As mentioned before Landauer formula, equation (6.1), can be used to calculate the transmitted current I as a function of the bias voltage, V_{ds}, applied between the source (left reservoir) and drain (right reservoir) for a CNFET, incorporating the effect of carrier transmission at the source/tube and drain/tube barriers in the WKB-computed transmission coefficient T, see equation (6.11).

Parameters $f(E)$ and $f(E-qV_{dS})$ in equation (6.1) are the Fermi distribution functions refer to the source and drain, respectively.

Hence using the Fermi-Dirac distribution definition they are defined to be

$$f(E)=f(E-b)=\frac{1}{1+\exp(\frac{E-b}{kT})} \tag{6.12}$$

$$f(E-qV_{dS})=f(E-(b-V_{dS}))=\frac{1}{1+\exp(\frac{E-(b-Vds)}{kT})} \tag{6.13}$$

Where, b is the distance between the Fermi level of the metal and mid band of the carbon nanotube channel.

As mentioned before electrons incident from the source reservoir with an energy E, has a transmission probability $T(E)$, see equation(6.11),to scatter through the carbon nanotube into the drain reservoir.

The integral in equation (6.1) theoretically extend from negative infinity to positive infinity, but the integrand contains $f(E)$ - $f(E-qV_{DS})$: the difference between the Fermi functions in the two contacts which is non-zero only from $f(E)$ to $f(E-qV_{DS})$ and a few kT on either side.

At some points, for low energies, $T(E)$ becomes zero when at another point, for high energies, $f(E)$ or $f(E-qV_{dS})$ (the Fermi distribution functions) becomes zero. These are the practical limit of the integral.

Here we calculated electron contribution to the current separately, this gives a lower limit of the conduction band edge for the electron current, and an upper limit of around 20 or 30kT above the highest contact Fermi level at the upper limit.

By putting $T(E)$, $f(E-b)$ and $f(E-(b-Vds))$ values in the Landauer formula, equation (6.1), current between source and drain can be calculated.
Figure 6-5 shows plots of equation (6.1) as a function of V_{ds}, from 0 to 0.7 V.
The difference between the Fermi level, E_F, of the metal contact and conduction band is assumed to be 0.05 eV and $\Phi_S=\Phi_D$ is set to 4.5 eV.
Therefore using the following parameters in to the (6.6) and (6.11) the transmission coefficients of the two end of the tube can be calculated.
Having b= 0.05 eV, c=4 nm, $m^* = 0.06 \times 9.11 \times 10^{-31} kg$,
V_0=0.3 eV, $h = 4.135 \times 10^{-15} eV.s$

We can find

$$T1(E) = \exp\{-3.82 \times 10^{-9} (0.35 - E)^{1.5}\}$$

$$T2(E) = \exp\{\frac{-1.33 \times 10^{-9}}{0.35 - Vds} [(0.35 - Vds - E)^{1.5} - (0.35 - Vds - 2E)^{1.5}]\}$$

At the same time equation (6.12) and (6.13) become

$$f(E-b) = f(E-0.05) = \frac{1}{1 + \exp(\frac{E-0.05}{kT})}$$

$$f(E-(b-Vds)) = f(E-(0.05-Vds)) = \frac{1}{1 + \exp(\frac{E-(0.05-Vds)}{kT})}$$

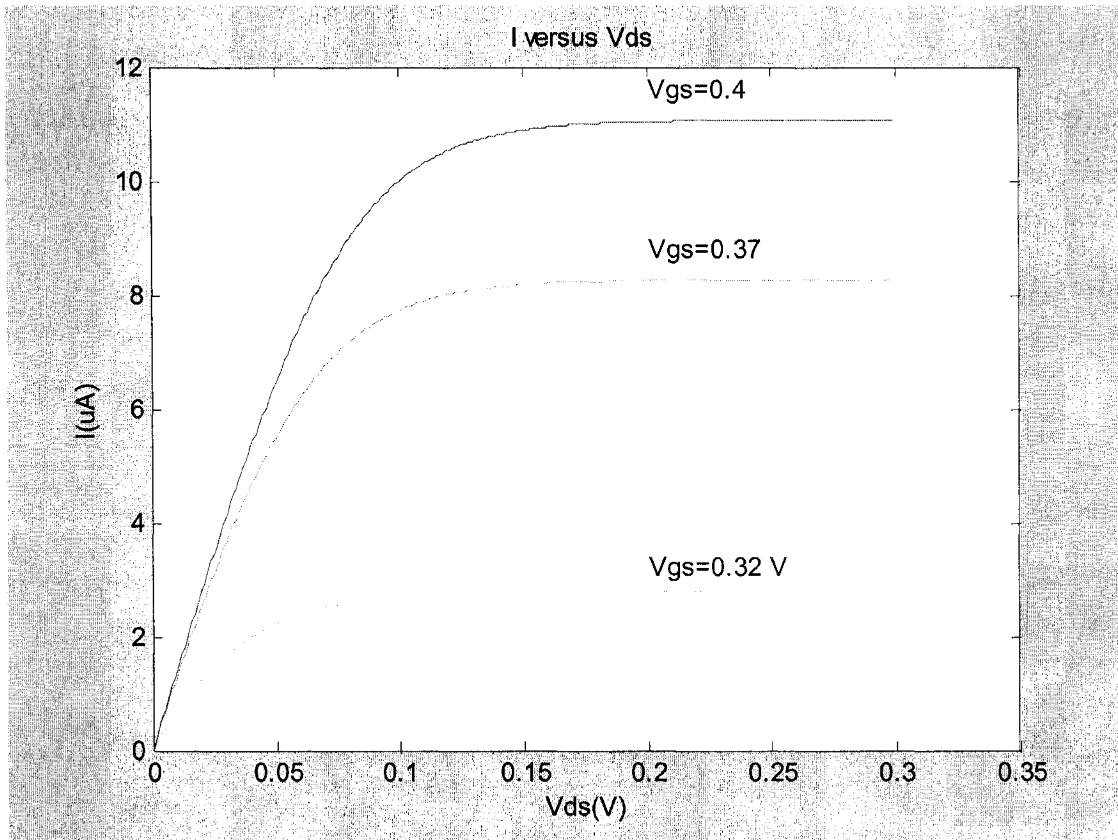

Figure 6-5: The computed I_d vs. V_{ds} characteristic with gate biases Vgs=0.32-0.37 V, 0.4 V for CNFET.

Figure 6-5 confirms the evolution of the drain characteristics and it can be seen that the ballistic CNFET show similar I-V characteristics to the ballistic MOSFETs, only the channel conductance is quantized in the case of CNFET. For a CNFET the saturation drain current is dependent of the drain-to-source voltage and work functions of the source/drain reservoirs.

At the same time for a constant voltage between source and drain, by increasing the gate voltage we can have more electrons to tunnel through the barrier and consequently, as can be seen in Figure 6-6, more current can be obtained. This can suggest that the performance of the CNFET can be improved by better gate electrostatics, for example, higher dielectric constant and thinner dielectric can improve the gate capacitance and can result in higher current between source and drain (I_{ds}).

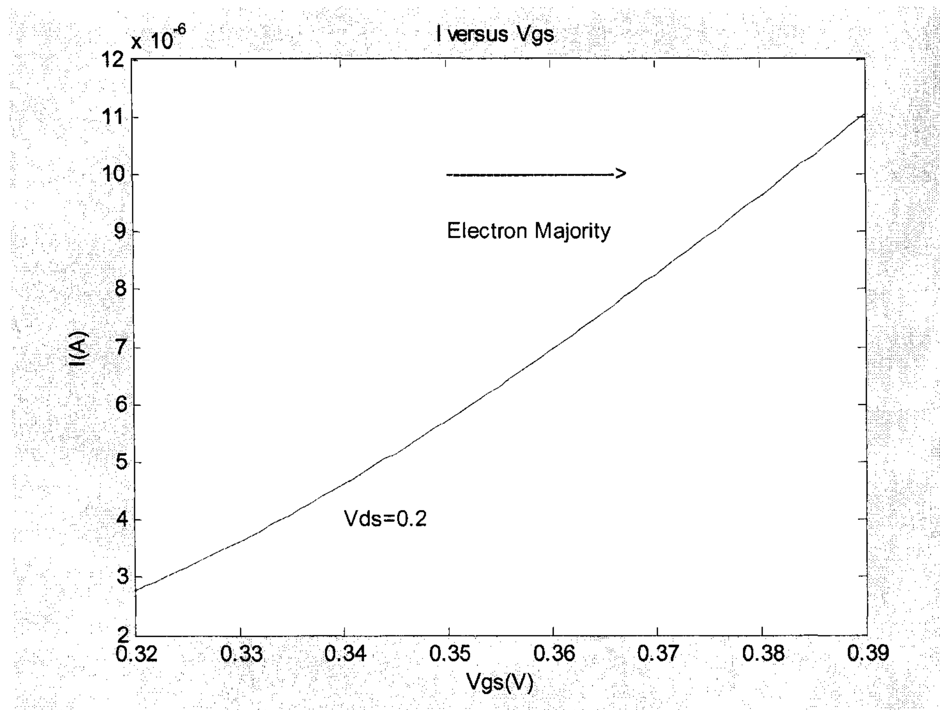

Figure 6-6: Current Characteristic of carbon nanotube for CNFETS at non-equilibrium when V_{ds}=0.2 v and V_{gs} changes from 0.32 to 0.39 volts.

Figure 6-7 shows the experimental results that were obtained by IBM research group. By comparing the theoretical and experimental results, Figure 6-5 and 6-7, it can be seen that the theoretical values are significantly larger in magnitude. The reason is that we assumed a perfect gate controlled electrostatics which means that we assumed the exact value of the gate voltage in our calculations. At the same time we ignored internal source/tube- and drain/tube-barriers in the WKB-computed transmission coefficient, *T*. Getting a significant higher current due to the assumption of ideal contacts at source and drain ends and better gate electrostatics can suggest the possibility to improve the performance by better device design.

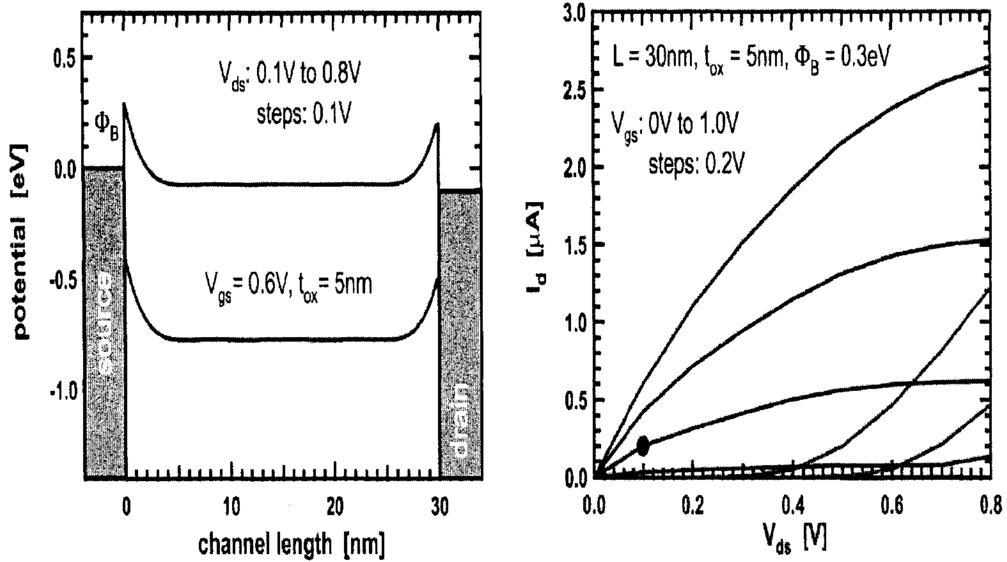

Figure 6-7: Switching in carbon nanotubes in CNFETS, linear region for small V_{ds} in the output characteristics and saturation for large enough V_{ds}. (experimental results) [2]

It is important to mention that increase in V_{ds} causes a spike to appear in the valence band profile at the drain. This will allow hole tunneling to occur and can increase the magnitude of the current because the total current considering both hole and electron current is $I=I_n + I_p$; however, using a noble metal with high work function and good wetting interactions with nanotubes, can greatly reduces or eliminates the barriers for transport through the valence band of the nanotubes [41].

Chapter 7

Conclusions, Contributions

7.1. Conclusions

Industry continues to scale down current semiconductor transistors .At the same time with the reduction of the size, physical restrictions become the issue and are difficult to surpass.

To aid the current miniaturization of transistors many technologies are being considered. Because of their unique properties, carbon nanotubes have a promising potential to aid in scaling. They can have different energy band gaps depending on their chirality and diameter and because of that they have properties ranging from metallic to semiconducting. Semiconducting carbon nanotubes can be used as the channel in transistors.

Most present CNT researches are related to the growth and properties of nanotubes; the work presented in this thesis displays their potential within carbon nanotube field effect transistor. The properties of CNTs have been discussed and it has been shown that CNFET transistor characterization has a potential to outperform the current silicon technology transistors.

The concentration of this work has been on a proposed model of carbon nanotube field effect transistor formed with a (16, 0) intrinsic carbon nanotube (zigzag nanotube) with the radius

R_{cn}=0.63 nm, and length of L_{cn}=100 nm.

For the equilibrium condition, the carrier concentrations in valence and conduction bands were found by allowing the local electrostatic potential to rigidly shift the carbon density of states. It has been shown that the charge density of the nanowire channel is determined by the electrostatic environment rather than the contact properties.

Two graphs with different approaches to the charge equation (with and without using Maxwell-Boltzmann approximation) show similar results. This suggests that the Maxwell-Boltzmann approximation can be used as a good estimation for determining the carbon nanotube charge for the mid band of the nanotube at low voltages.

The electrostatics of CNFETs was explored by self-consistently solving the Poisson equation in one dimension with the equilibrium carrier concentration. The two graphs of conduction energy band near the source end of the carbon nanotube channel of CNFET that were obtained by different approaches to the charge equation (with and without using Maxwell-Boltzmann approximation) are different suggesting that Maxwell-Boltzmann approximation is not a good estimation for determining the energy band diagrams even for low voltages.

The CNFET I-V characteristic has been estimated by applying voltage to the source/drain contacts and considering the triangle shape for Schottky barriers. CNFET Schottky barriers are formed between the metal contacts at source/drain and semiconducting carbon nanotube and current is mainly dominated by tunneling through these barriers. The electrostatics of these potential barriers are controlled by the applied voltage at source and drain. The drain voltage can diminish the barrier at its contact and this is where saturation happens.

The result confirms the evolution of the drain characteristics and it can be seen that ballistic CNFETs show similar I-V characteristics to the ballistic MOSFETs. The drain current saturation displayed in the output characteristics occurs when the drain bias is large similar to the same situation in ballistic MOSFET.

The on-current of the computed ballistic CNFET are well above the values that was obtained experimentally due to the assumption of ideal metal-nanotube contacts, ballistic channel transport and rough approximation of the Schottky barriers and better gate controlled electrostatics. The current can vary among transistors depending on the source and drain variation suggesting possible improvement of the CNFETs performances by better device design.

For a constant voltage between source and drain, we have shown that by increasing the gate voltage we can have more electrons to tunnel through the barrier and consequently more current can be obtained.

This can suggest that the performance of the CNFET can be improved by better gate electrostatics, for example, higher dielectric constant and thinner dielectric can improve the gate capacitance and can result in higher I_{ds}.

In certain aspects carbon nanotube transistors are competitive with Silicon MOSFETs and can be further improved by detailed understanding of the physics in nanostructures as was explained in this thesis. Although the carbon nanotube technology is very young but its promising I-V characteristic provides great hope for future circuit designs and can open many new opportunities for digital circuit designers.

7.2 Contributions

The main contributions of this research work are listed as follows:

1) In this thesis we developed an analytical theory for nanometer-size field-effect transistor that although it is used here for CNFET it can be used in general for any nanowire field effect transistor.

2) Charge density versus Gate voltage graph at the mid band of the carbon nanotube for both electrons and holes confirms that by increasing the gate voltage , the Fermi level gets closer to the conduction band of the nanotube and the electron density increases exponentially vs. gate voltage where at the same time the hole density decreases exponentially.

3) Comparing two graphs of electron density at the mid band of the carbon nanotube channel with different approaches to the charge equation shows the similar result suggesting that Maxwell-Boltzmann approximation can be used as a good estimation for determining the carbon nanotube charge for the mid band of the nanotube for low voltages.

4) Charge density at source and drain end of the carbon nanotube versus Schottky barrier height graph confirms that the electron density increases as the Schottky barrier bending decreases.

5) The electrostatics of CNFET was explored by self-consistently solving the Poisson equation in one dimension with the carrier statistics. Unlike the bulk contacts we can see that the charge density on the nanowire depends critically on the electrostatic environment rather than the properties of the metal contacts because of one dimensional contact between the nanowire and metal. This can suggest that reducing the gate oxide thickness would improve the transistor performance.

6) The simulation result shows that the I-V characteristic of the CNFET is similar to the I-V characteristic of the MOSFET. The drain saturation displayed in the output characteristic occurs when the drain bias is large similar to that of the MOSFET.

7) By getting a significant larger current than the experiment it can be seen that the performance of the CNFET can be improved with better gate electrostatics. The on-current of the computed ballistic CNFET are well above the values currently being obtained experimentally due to our assumption of ideal metal-nanotube contacts, ballistic channel transport and perfect gate controlled electrostatics suggesting possible improvement of the CNFET performances by better device design .

8) Current Characteristic of carbon nanotube for CNFETS at non-equilibrium for a constant source/drain voltage and different gate voltage shows that more electrons can tunnel through the barrier and consequently more current can be obtained. This can suggest that the performance of the CNFET can be improved by better gate electrostatics, for example, higher dielectric constant and thinner dielectric can improve the gate capacitance and can result in higher I_{ds}.

9) This work confirms the evolution of the drain characteristics- which is believed to dominate the transport in nanostructures- in a user friendly and understandable modeling of

Schottky barriers of CNFET. Although the Carbon nanotube technology is very young but its promising I-V characteristic provides great hope for future circuit designs and can open many new opportunities for digital circuit designers.

References:

[1] www.intel.com[May 2005]

[2] www.nanohub.org [September 2005]

[3] www.zurich.ibm.com[October 2005]

[4] www.scientificamerican.com [October 2005]

[5] S. Woedtke, Ph.D. thesis, Inst. f. Exp. u. Ang. Phys. der CAU Kiel, (2002).

[6] Hamers Research Group website (hamers.chem.wisc.edu).[November 2005]

[7] Mark Robertus Buitelaar, PhD thesis, Basel University,''Electron Transport in Multiwall Carbon Nanotubes, (2004).

[8] M. Dresselhaus, G. Dresselhaus, P. Eklund, and R. Saito, "Carbon nanotubes," Physics Web Online.

[9] Saito, Y. "Nanoparticles and filled nanocapsules". Carbon 33, 979-988, 2005.

[10] P. G. Collins, M. S. Arnold, and Ph. Avouris, "Engineering carbon nanotubes and nanotube circuits using electrical breakdown," Science, vol. 292, pp. 706—709, Apr. (2001).

[11] R. Martel, T. Schmidt, H. R. Shea, T. Hertel, and Ph. Avouris, Appl. Phys.Lett. 73, 2447 (1998).

[12] S. Heinze, J. Tersoff*, R. Martel, V. Derycke, J. Appenzeller, and Ph. Avouris, "Carbon Nanotubes as Schottky Barrier Transistors",Appl.Phys. Lett. 80 , 2773 (2002).

[13] J.Appenzeller, IBM T.J. Watson Research Center, "Electronic Transport in Semiconducting Carbon Nanotubes". Perdue University's Seminar.

[14] François Léonard and J. Tersoff,'' Role of Fermi-Level Pinning in Nanotube Schottky Diodes''. Phys. Rev. Lett. 84, 20 (2000).

[15] L.C. Castro, D.L. John and D.L. Pulfrey, ``Towards a compact model for Schottky-barrier nanotube FETs", Proc. IEEE COMMAD-02, 303-306, (2003).

[16] M. S. Dresselhaus, G. Dresselhaus, and Ph. Avouris, "Carbon Nanotubes: Synthesis, Structure,Properties, and Applications", vol. I, Springer, New York, (2001).

[17] T. W. Ebbesen and P. M. Ajayan, "Large-scale synthesis of carbon nanotubes," Nature, vol. 358, pp. 603—605, (1992).

[18] A. Thess, R. Lee, P. Nikolaev, H. Dai, P. Petit, J. Robert, C. Xu, Y.H. Lee, S.G. Kim,D.T. Colbert, G. Scuseria, D. Tomanek, J.E. Fischer, and R.E. Smalley, "Crystalline ropes of metallic carbon nanotubes," Science, vol. 273, pp. 483—487, (July 1996).

[19] R.Saito, G.Dresselhaus, M S Dresselaus, Physical Properties of Carbon Nanotubes, Imperial College press, first edition (2002).

[20] Sang-MoKoo,Monica D Edelstein,Qiliang Li, Curt ARichter and Eric M Vogel, "Silicon nanowires as enhancement-mode Schottky barrier field-effect transistors"Nanotechnology 16,1482–1485, (2005).

[21] D.L. John, L.C. Castro and D.L. Pulfrey, "Quantum Capacitance in Nanoscale Modeling", J. Appl. Phys., vol. 96, 5180-5184, (2004).

[22] Powell and Crasemann, Quantum Mechanics. Addison-Wesley Pub, first edition.

[23] Y. Zhang, T. Ichihashi, E. Landree, F. Nihey, S. Iijima., "Heterostructures of Single-Walled Carbon Nanotubes and Carbide Nanorods" , Science 285, Vol. 285. no. 5434, pp. 1719 – 1722, (1999).

[24] K. Natori,"Field-Effect Modulation of the Conductance of Single Molecules'',J. Appl. Phys. **76**, 4879(1994).

[25] S.Datta, Nanoscale device modeling: the Green's function method,Available online at http://www.idealibrary.com (2005)

[26] . Kong, C. Zhou, A. Morpurgo, H. T. Soh, C. F. Quate, C. Marcus, and H. Dai, "Synthesis, integration, and electrical properties of individual single-walled carbon nanotubes," Appl. Phys. A69, 305-308 (1999).

[27] Joerg Appenzeller (IBM) presentation slides at Perdue university (www.nanohub.org), (2005).

[28] Sander J. Tans, Alwin R. M. Verschueren, and Cees Dekker "Room-temperature transistor based on a single carbon nanotube." Nature 393, pp.49-51 (1998).

[29] P. G. Collins and Ph. Avouris, "Nanotubes in electronics." Scientific American, pp. 62—69,(Dec. 2000).

[30] A. Javey, Q. Wang, A. Ural, y. Li, and H. Dai, "Carbon nanotube transistor arrays for
multistage complementary logic and ring oscillators," Nano Letter, vol. 2, no. 9, pp.929—932, (2002).

[31] S.M.Sze, Physics of Semiconductor Devices. Second edition.

[32] Donald A.Neaman, Semiconductor Physics and Devices, Basic Principles, third edition.

[33] U. Ascher, R. Mattheij, and R. Russell, "Numerical Solution of Boundary Value Problems for Ordinary Deferential Equations", SIAM, Philadelphia, PA, (1995).

[34] Tezaswi Raja, Vishwani D. Agrawal, Michael L. Bushnell:"A Tuturial on the Emerging Nanotechnology Devices". VLSI Design: pp. 343-360(2004).

[35] S. Heinze, J. Tersoff, R. Martel, V. Derycke, J. Appenzeller, and Ph. Avouris,"Carbon Nanotubes as Schottky Barrier Transistors," Phys. Rev. Lett., vol. 89, no.10, p. 106801, 2002.

[36] Jing Guo, Sebastien Goasguen, M. S. Lundstrom and S. Datta , "Metal-Insulator-Semiconductor Electrostatics of Carbon Nanotubes." Appl. Phys. Lett., Vol. 81, No. 8, pp. 1486-1488. (19 Aug. 2002).

[37] M. P. Anantram, S. Datta and Y. Xue, "Coupling of carbon nanotubes to metallic contacts." Phys. Rev. B, vol. 61, p. 14219 (2000)

[38] Supriyo Datta, Electronic Transport in Mesoscopic Systems - Cambridge University Press, 1995, Paperback Edition (1997).

[39] J. Guo, M. Lundstrom and S. Datta, "Performance Projections for Ballistic Carbon Nanotube Field-Effect Transistors", Applied Physics Letters, vol. 80, no. 17, p. 3192, (2002).

[40] J. Guo, J. Wang, E. Polizzi, Supriyo Datta and M. Lundstrom and H. Dai, "Electrostatics of Nanowire Transistors," IEEE Transactions on Nanotechnology, vol. 2, p. 329, (Dec. 2003).

[41] A. Javey, J. Guo, Q. Wang M. Lundstrom and H. Dai., "Ballistic Carbon Nanotube

Field-Effect Transistors," Nature, vol. 424, pp. 654-657, 2003.

[42] F. Leonard and J. Tersoff, "Novel Length Scales in Nanotube Devices," *Phys. Rev. Lett.*, vol. **83**, pp. 5174-5177, 1999.

[43] D.L. John, L.C. Castro, J.P. Clifford and D.L. Pulfrey, ``Electrostatics of coaxial schottky-barrier nanotube field-effect transistors", IEEE Trans. Nanotech., vol.2, pp. 175-180, (2003).

[44] D.L. John, L.C. Castro, P.J.S. Pereira and D.L. Pulfrey, "A Schrödinger-Poisson Solver for Modeling Carbon Nanotube FETs," Proc. NSTI Nanotech., vol.3, pp. 65-68, (2004).

[45] L.C. Castro, D.L. John and D.L. Pulfrey, ``Carbon nanotube transistors: an evaluation", Proc. SPIE Conf. Device and Process Technologies for MEMs, Microelectronics, and Photonics III, vol. 5276,pp. 1-10, (2004).

[46] J.P. Clifford, D.L. John, L.C. Castro, and D.L. Pulfrey, "Electrostatics of Partially Gated Carbon Nanotube FETs," IEEE Transactions on Nanotechnology, vol.3, pp.281-286, (2004).

[47] A. Rahman, J. Guo, S. Datta, and M. Lundstrom, "Theory of Ballistic Transistors," IEEE Transactions on Electron Devices, vol. 50, p. 1897, (2003).

[48] J. Guo, Supriyo Datta and M. Lundstrom, "A Numerical Study of Scaling Issues for Schottky Barrier Carbon Nanotube Transistors," IEEE Transactions on Electron Devices, vol. 51, p. 172, (2004).

[49] Z. Ren, R. Venugopal, S. Datta, M. Lundstrom, D. Jovanovic, and J.Fossum, "The ballistic nanotransistor: A simulation study," Int. Electron Devices Meeting Tech. Dig., San Francisco, CA, pp. 715-718 ,(2000).

Appendix A

A.1 Matlab Code for Potential profile of the Carbon Nanotube field effect Transistors (Using Maxwell-Boltzmann approximation).

```
function bratubvp
options = bvpset('stats','on');
solinit = bvpinit(linspace(0,6,5),[4 0.15]);
sol1 = bvp4c(@bratuode,@bratubc,solinit,options);

fprintf('\n');

% Change the initial guess to converge to a different solution.
solinit = bvpinit(linspace(0,6,5),[0.4 0]);
sol2 = bvp4c(@bratuode,@bratubc,solinit,options);

Figure
plot(sol1.x,sol1.y(1,:),sol2.x,sol2.y(1,:))
%title('Schottky barriers tend to have a triangle shape in one dimension-nanometer size
of the CNT without using WKB approximation')
xlabel('z(nm)')
ylabel('V(z)')
-----------------------------------------------------------------------------------------------
function dydx = bratuode(x,y)
%BRATUODE  ODE function for the exercise of Example 1 of the BVP tutorial.
dydx = [  y(2)
        0.02*exp(-y(1)/0.0259)];
```

```
function res = bratubc(ya,yb)
%BRATUBC  Boundary conditions for the exercise of Example 1 of the BVP tutorial.


res = [ya(1)-0.5
     yb(1)];
```

A.2. Matlab Code for Potential profile of the Carbon Nanotube field effect Transistors (Without Using Maxwell-Boltzmann approximation).

```
%Form a guess structure consisting of an initial mesh of ten equally spaced points in
[0,5nm]
% and a guess of constant values and with the command
solinit = bvpinit(linspace(0,5,10),[0 0.1]);

%Now solve the problem with
sol = bvp4c(@twoode,@twobc,solinit);

%Evaluate the numerical solution at 100 equally spaced points and plot  with
x = linspace(0,5);
y = deval(sol,x);
plot(x,y(1,:));
xlabel('z(nm)')
ylabel('V(z)(eV)')

%----------------------------------------------------------------------------------------------------
function dydx = twoode(x,y)
  F = @(E)(E.^(-0.5).* ( 1 ./ (1 + exp(E + y(1))/(0.0259) ) ) );
  I = quad(F,0,5);
  J=0.91.*I
  dydx = [ y(2)
```

```
        J];

%--------------------------------------------------------------------------------------------
function res = twobc(ya,yb)
 res = [ ya(1) - 0.5
        yb(1) - 1e-5];
```

A.3 Matlab Code for the computed I_d vs V_d characteristic with gate biases a parameter Vgs=0.32 V, 0.37,0.4 V for carbon nanotube channel.

```
n=1;
%b=0.07 and vgs=0.39
for v = 0:0.001:0.3
   V(n) = v;
   F = @(E)(((4*1.6*10^(-19))/(4.135*10^(-15))).*(exp(-4.78*10^(-9).*(0.37-
E).^(1.5)).*exp([-1.3*10^(-9).*((0.37-v-E).^(1.5)-(0.37-v-2.*E).^(1.5))]./(0.37-
v))).*((1./(1+exp((E-0.07)./0.0259)))-(1./(1+exp((E-(0.07-v))./0.0259)))));
   I(n) = quad(F,0,0.2);
   n=n+1;
end
I=I*10^(6)
plot(V,I)
text(0.2,1.16*10,'Vgs=0.4')


   hold on

   clear all;
n=1;
```

```
%b=0.05 and vgs=0.37
for v = 0:0.001:0.3
   V(n) = v;
   F = @(E)(((4*1.6*10^(-19))/(4.135*10^(-15))).*(exp(-3.82*10^(-9).*(0.35-
E).^(1.5)).*exp([-1.3*10^(-9).*((0.35-v-E).^(1.5)-(0.35-v-2.*E).^(1.5))]./(0.35-
v))).*((1./(1+exp((E-0.05)./0.0259)))-(1./(1+exp((E-(0.05-v))./0.0259)))));
   I(n) = quad(F,0,0.2);
   n=n+1;
end
I=I*10^(6)
plot(V,I,'red')
text(0.2,0.88*10,'Vgs=0.37')

 hold on
 clear all;
n=1;
%b=0 vgs=0.32
for v = 0:0.001:0.3
   V(n) = v;
   F = @(E)(((4*1.6*10^(-19))/(4.135*10^(-15))).*(exp(-1.1*10^(-9).*(0.3-
E).^(1.5)).*exp([-1.3*10^(-9).*((0.3-v-E).^(1.5)-(0.3-v-2.*E).^(1.5))]./(0.3-
v))).*((1./(1+exp((E)./0.0259)))-(1./(1+exp((E-(-v))./0.0259)))));
   I(n) = quad(F,0,0.2);
   n=n+1;
end
I=I*10^(6)
plot(V,I,'green')
text(0.2,0.32*10,'Vgs=0.32 V')
xlabel('Vds(V)')
ylabel('I(uA)')
title('I versus Vds')
```

A.4 Matlab Code for electron density versus Gate voltage when the source/drain voltage is zero.

```
x=0:0.01:0.25;
Ecmid=0.3-x;
y=56.94*10^(4)*exp(-Ecmid/0.0259);
plot(x,y)
xlabel('Vgs(V)')
ylabel('Qmidband(e/cm)')
text(0.2,5*10^(4),'Vds=0')
title('Charge vs Gate voltage Curve')
```

A.5 Matlab Code for hole density versus Gate voltage when the source/drain voltage is zero.

```
x=0:0.01:0.25;
Evmid=-0.3-x;
y=56.94*10^(4)*exp(Evmid/0.0259);
plot(x,y)
xlabel('Vgs(V)')
ylabel('Qmidband(h/cm)')
text(0.02,4,'Vds=0')
title('Charge vs Gate voltage Curve')
```

A.6 Matlab Code for he Schottky barrier height for electrons and holes vs. charge density where Maxwell-Boltzmann approximation is applicable.

```
x=0:0.001:0.3;
y=1.6*10^(6)*exp(-x/0.0250)-0.23*exp(x/0.0259);
plot(y,x)
ylabel('qV(z)(ev)')
xlabel('Density[/m]')
title('The Schottky barrier height for electrons and holes vs. charge density')
```

A.7 Matlab Code for electron density versus Gate voltage when the source/drain voltage is zero.

```
n=1;
for x = 0:0.001:0.3
   X(n)=x
   v=0.3-x;
  F = @(E)(E.^(-0.5).* ( 1 ./ (1 + exp((E+v)./(0.0259)) ) ) );
  I(n) = quad(F,0,10);
n=n+1;
end
I=I.*199.63*10^(4)
plot(X,I)
xlabel('Vgs(V)')
ylabel('Qmidband(e/cm)')
text(0.15,1*10^(5),'Vds=0')
title('without Maxwell-Boltzmann approximation approach')
```

A.8 Matlab Code for the computed I_d vs V_{gs} characteristic with source/drain biases a parameter Vds=0.2 V for carbon nanotube channel.

```
b=0:0.001:0.09
vgs=0.32+b
vds=0.2
n=1;
for b =0:0.001:0.07
   B(n) = b;
   V(n)=0.32+b
   F = @(E)(((4*1.6*10^(-19))/(4.135*10^(-15))).*(exp((-1.33*10^(-9)).*((0.3+b-
E).^(1.5))./(0.3+b)).*exp([-1.3*10^(-9).*((0.3+b-0.2-E).^(1.5)-(0.3+b-0.2-
2.*E).^(1.5))]./(0.3+b-0.2))).*((1./(1+exp((E-b)./0.0259)))-(1./(1+exp((E-(b-
0.2))./0.0259)))));
```

```
  I(n) = quad(F,0,0.2);
  n=n+1;
end

plot(V,I)
xlabel('Vgs(V)')
ylabel('I(A)')
title('I versus Vgs')
text(0.34,4*10^(-6),'Vds=0.2')
text(0.35,9*10^(-6),'Electron Majority')
text(0.35,10*10^(-6),'------------------------->')
```